The Thesis Committee for Stephen Vargo Williams
Certifies that this is the approved version of the following thesis:

Development of a Dynamic Torsion Testing System

APPROVED BY
SUPERVISING COMMITTEE:

Supervisor: _____
Krishnaswamy Ravi-Chandar

_____
Kenneth M. Liechti

Development of a Dynamic Torsion Testing System

by

Stephen Vargo Williams, B.S.M.E.

Thesis

Presented to the Faculty of the Graduate School of

The University of Texas at Austin

in Partial Fulfillment

of the Requirements

for the Degree of

Master of Science in Engineering

The University of Texas at Austin

May 2014

Acknowledgements

I would like to thank my supervisor Professor K. Ravi-Chandar for providing financial support for my research and mentoring my studies at the University of Texas at Austin.

I also extend my appreciation to Joseph Pokluda, Pablo Cortez, Travis Crooks and Ricardo Palacios for their extensive help and diligent work in fabricating and instrumenting the experimental apparatus.

I would like to thank my fellow graduate students for making these years in graduate school so memorable: Ian, Bobby, Shravan, Nebiyu, Anand, Sundeep, Steven, Sasha, Gary, Alex, Andrew, Khai, Chenglin, John and many more.

I would also like to express my gratitude to my family for supporting me through graduate school: my mother Sherri, my brother Thomas, my sister Veronica, and Olinda.

Abstract

Development of a Dynamic Torsion Testing System

Stephen Vargo Williams, M.S.E.

The University of Texas at Austin, 2014

Supervisor: Krishnaswamy Ravi-Chandar

The aim of this thesis is to design and build a torsional Kolsky bar apparatus for testing cylindrical specimens in torsion at high strain-rates. In addition to well-established designs, this testing apparatus will include a conical mirror combined with a high speed camera that allows time-resolved optical observation of the shear deformation on the surface of the specimen. The basic design of a Kolsky bar consists of a loading bar, input bar, specimen, and output bar. The experiment is conducted by storing torque in the loading bar and then releasing the torque by breaking the clamp and sending a shear wave pulse through the apparatus into the specimen. This shear wave pulse is monitored by strain gages mounted on the input and output bars. Analysis of the strain waves in the input and output bar is used to extract the shear stress - shear strain profile of the specimen. Several experiments were conducted on 6061-O and 1100-O aluminum with wall thicknesses ranging from 0.3 to 1.5 mm.

Table of Contents

List of Figures

Chapter 1: Introduction

The response of materials subjected to large deformation rates is required for applications involving impact or shock loading such as the design of munitions, armor, and high-speed machining among many others. For many common materials, there is a strain rate dependent response that can only be obtained through experiments conducted at the corresponding strain rate. The results from these experiments can then be incorporated into computational models for the relevant applications.

The Kolsky bar is an experimental apparatus that can be used to deduce dynamic material properties through the use of longitudinal elastic wave propagation in rods. There are tension, compression and torsion variants of this device, which provide insight into material behavior under high strain rate loading of the respective loading type. There are several advantages to the dynamic torsion test over the tension and compression tests. Torsion loading can produce a nearly homogeneous state of pure shear when used in conjunction with a thin-walled tubular specimen. The homogeneous stress state avoids introducing geometric instabilities at large shear strains such as necking found in the tension test. Higher average strain rates can be obtained through the use of shorter gage length specimens than can be utilized in the tension and compression tests due to the distortion introduced by end boundary conditions. (Lindholm, 1980)

The torsional Kolsky bar consists of two long bars that are free to rotate, with a short thin walled specimen placed between them. A test is conducted by isolating a section of the first bar, denoted as the incident bar, using a clamp and applying a torque that is stored as shear strain. The clamp is then released which sends a torsional wave

pulse through the rest of the incident bar that is transmitted into the specimen and then passes to the second bar, denoted as the output bar. At the interface between the incident bar and the specimen there is both a reflected wave and a transmitted wave. The specimen then deforms plastically, absorbing some energy contained by the transmitted wave and the remainder passes through to the output bar. The incident, reflected and transmitted waves are measured by strain gages placed on the incident and output bars respectively. The amplitude of the torsion wave is significantly greater than the amount required to yield the specimen so a majority of the energy is reflected, causing one end of the specimen to rotate with a high angular velocity with respect to the other end. This high rate of deformation generates a large uniform shear strain throughout the specimen. (Graff, 1975)

The addition of high speed imaging to the torsional Kolsky bar allows observation of non-uniform phenomena in the specimen during the loading stage. Through the use of a cone-mirror, the entire surface of the specimen can be observed by a single camera.

1.1 Literature Review

There are multiple approaches to dynamic torsion testing that can be selected based on the desired range of strain rates. Lindholm (1980) describes three main testing archetypes that are defined by the method of loading employed. The different mechanisms include: a rotary flywheel, a hydraulic or pneumatic torsional actuator, and the torsional Kolsky bar. The rotary flywheel operates by spinning the flywheel up to the desired speed and quickly coupling it to the thin-walled specimen. A primary design

concern of this apparatus is matching the torsional stiffness of the flywheel and the specimen to effectively transmit the torque and avoid extraneous torsional vibrational feedback. A device of this style was constructed by Culver (1972) and obtained shear strain rates up to 300 s^{-1} in alloys with ultimate strengths up to 200 MPa. The hydraulic actuator operates by accumulating hydraulic fluid until it ruptures a metal diaphragm at a set pressure and flows into the actuator producing the high rotational velocity that is transmitted into the specimen. Lindholm (1980) developed and refined a device of this type to produce variable strain rates up to 500 s^{-1} in copper specimens.

The torsional Kolsky bar distinguishes itself by generating strain rates up to 10000 s^{-1} depending on the configuration of the bar and specimen. The Kolsky bars and specimen geometries developed by Duffy (1988) and Gilat (2000) serve as the inspiration for the design used in this study. There have been several iterations of the measurement system and loading mechanism used to generate torque in Kolsky bars.

The method used by Duffy (1971) was to fire a detonator with explosive leader bars to quickly twist the input bar and generate strain rates up to 800 s^{-1}. This device contained the typical input and output bar components but was oriented vertically. The specimens used were thick-walled tubes with a narrow diameter in the middle of the length that served as the active part. These specimens were coupled to the input and output bars through an epoxy adhesive. The explosive loading source produced a relatively noisy input that required a pulse smoother adapter in order to create a usable input for the specimen. The pulses generated by this system were relatively short and only produced shear strains of 5 percent in aluminum 1100-O specimens.

In a later experiment, Marchand and Duffy (1988) observed the formation of adiabatic shear bands in HY-80 steel through the addition of high speed imaging. To accomplish this, Duffy placed three short exposure cameras around the specimen and triggered them simultaneously. The Kolsky bar used in this experiment followed the more conventional configuration of a quasi-statically loaded clamped bar and horizontally placed input and output bars. The specimen geometry for this experiment consisted of a thin-walled tube with hexagonal flanges that were mated to matching sockets on the input and loading bars. With this combination of Kolsky bar and specimen, Duffy (1988) generated strain rates around 3300 s^{-1} over a long duration that produced a strain of 60 percent.

Gilat (1988) built a Kolsky bar that generated torque through the use of a loading wheel turned by a pulley in a clamped section of the input rod which generated strain rates around 2400 s^{-1}. Gilat also modified the input bar to consist of two sections with different cross-sectional areas. This generated a strain pulse with an initially high strain rate followed immediately by a strain rate one tenth the initial magnitude. This modification allowed Gilat to study the effects of reducing the strain rate during high-rate plastic deformation on 1100-O aluminum specimens.

Gilat (2000) later modified the Kolsky bar to generate strain rates above 10^4 s^{-1} through the use of an extremely short specimen. The specimens used for the highest strain rates had a gage length of only 0.1524 mm which required electrical discharge machining. The results from this experiment show that the strain-rate dependent yield strength of 1100-O aluminum continues to increase at higher strain rates. To improve the

quality of the incident wave, Gilat modified the clamping system to be self-equilibrating through the use of a suspended hydraulic C-clamp.

1.2 Outline of present study

The motivation for this study is to develop a system to conduct dynamic torsional testing. To this end, a torsional Kolsky bar and cone-mirror imaging system will be constructed to investigate the behavior of 6061-O and 1100-O aluminum under high strain rate shear loading. The thesis is organized as follows: Chapter 2 contains an explanation of the principle of operation of the Kolsky bar. Chapter 3 contains a description design and assembly of the testing apparatus. Chapter 4 contains the results and analysis of the experiments. Finally, Chapter 5 summarizes the conclusions of the study.

Chapter 2: Principle of Torsional Kolsky Bar

A split Hopkinson pressure bar is a testing apparatus used for acquiring dynamic inelastic material properties by applying the theory of longitudinal elastic wave propagation in rods. The original Hopkinson bar was developed by Bertram Hopkinson in 1914 utilizing a single bar and was later modified by Herbert Kolsky in 1949 to include two bars in series, becoming the split Hopkinson bar or Kolsky bar. The basic system contains two metallic bars with a specimen placed between them. A rectangular stress wave pulse is generated in the first bar and propagates through to the specimen. Upon reaching the specimen, the wave dynamically loads the specimen and splits into a reflected wave that passes back through the first bar and a transmitted wave that continues into the second bar. These incident, reflected, and transmitted waves are all recorded by strain gages placed on either side of the specimen on the two bars. From the recorded strain measurements, the dynamic stress-strain state of the specimen can be determined. A general schematic is shown in Fig 2.1. The theory and systems required for the operation of a torsional Kolsky bar are discussed in detail in this chapter.

2.1 Elastic Torsional Wave Propagation in Rods

The experiments performed use the concept of elastic torsional wave motion in rods to generate and measure the shear strains in the specimen. The governing equation for this analysis will be developed from strength of materials concepts following the method presented by Graff (1975). Consider a differential element of a rod subjected to

variable end torques as shown in Fig 2.2. Following Newton's second law, the equation of motion for the element becomes:

$$-T + \left(T + \frac{\partial T}{\partial x}dx\right) = \rho J dx \frac{\partial^2 \theta}{\partial t^2} \tag{2.1}$$

where ρ is the density and J is the polar moment of inertia of the rod. The equation then reduces to:

$$\frac{\partial T}{\partial x} = \rho J \frac{\partial^2 \theta}{\partial t^2} \tag{2.2}$$

The angle of twist, θ, is related to the torque through a kinematic relationship:

$$T = C \frac{\partial \theta}{\partial x} \tag{2.3}$$

The quantity C represents the torsional rigidity and is dependent on the second moment of area, J, and shear modulus, G, of the bar. For a bar with a circular cross-section $C = JG$. Substitute this relationship into the governing equation:

$$\frac{\partial}{\partial x}(JG \frac{\partial \theta}{\partial x}) = \rho J \frac{\partial^2 \theta}{\partial t^2} \tag{2.4}$$

For a rod of uniform cross-sectional area and material composition this equation becomes:

$$\frac{\partial^2 \theta}{\partial x^2} = \frac{\rho}{G} \frac{\partial^2 \theta}{\partial t^2} \tag{2.5}$$

The shear wave speed is defined as the square root of the shear modulus divided by the density of the material.

$$c_s = \sqrt{\frac{G}{\rho}} \tag{2.6}$$

This equation is commonly written in the form of the standard linear wave equation as:

$$\frac{\partial^2\theta}{\partial x^2} = \frac{1}{c_s^2}\frac{\partial^2\theta}{\partial t^2} \tag{2.7}$$

Eq. (2.7) serves as the governing equation for the torsional wave system and subsequent equations describing the transmission and reflections of waves throughout the system will be derived from this form.

2.2 Kolsky Bar Arrangement

The arrangement of the Kolsky bar is designed to produce the incident, reflected and transmitted torsional waves required for the experiment and analysis. In a general sense, the system is composed of an input and output bar with a specimen mounted between the two. More specifically, the input bar is split into an isolated clamped region where the torque is stored and the free region into which the torque is released. The clamped region is loaded through the use of a loading wheel attached at the left end of the input bar. A primary requirement for the design of the input bar is that the clamped region is significantly shorter than the unclamped section, usually around one fourth the length. This ratio of lengths allows for the measurement of the incident and reflected waves to occur independently. Another factor to consider is the diameter and cross section shape of the bar. The bar can be made from either a solid circular or tubular cross section and commonly has a diameter between one half and one inch depending on the available torque and material used. Aluminum is the most widely used material but steel and titanium have also been used. When selecting these material and geometric properties it is important to consider the angular velocity, $\dot{\theta}$, that can be generated for a given input torque, T, the relationship for which is expressed as:

$$\dot{\theta} = \mp \frac{T}{\rho J c_s} \tag{2.8}$$

for right and left going waves respectively.

To identify the maximum elastic torque that can propagate in the bar, the relationship with the shear yield stress, τ_Y, of the bar must be examined:

$$T_Y = \frac{\tau_Y J}{r} \tag{2.9}$$

Substituting this relationship into Eq (2.7) we obtain a description how the maximum angular velocity relates to the material properties of the bar:

$$\dot{\theta} = \frac{\tau_Y}{r\sqrt{\rho G}} \tag{2.10}$$

Using Eq. (2.10) the maximum angular velocities in a bar with a radius of 6.35 mm for each material are as follows: aluminum = 3.9e3 rad/s, steel = 2.9e3 rad/s, titanium = 6.2e3 rad/s. Even though its density and modulus are higher than that of Al alloys, Ti can generate a much larger rotation rate because if its high yield strength. For this experiment, however, the maximum torque available is limited by the design of the torqueing and releasing mechanism, and does not approach the shear yield strength of any of the aforementioned materials. Therefore, applying Eq. (2.8) to identify which material produces the greatest angular velocity at the design torque of 20 N·m yields: aluminum = 0.25 rad/s, steel = 0.08 rad/s, titanium = 0.15 rad/s.. This ratio of angular velocities will be constant for any torque up to 80 N·m, which corresponds to the yield strength of aluminum and is beyond the maximum torque carrying capacity of the clamp. This demonstrates that aluminum is the most suitable material for this application and explains its wide use in other Kolsky bars

The incident wave is generated by the sudden release of stored torque and is characterized by its rise time, magnitude, and duration. The torque magnitude of the incident wave should be significantly larger than the torque required to yield the specimen. It is desired that the incident wave approximate a square wave profile with a short rise time on the order of 40 microseconds and relatively constant magnitude with a sharp cutoff. This requirement heavily influences the design of the clamp and release mechanism to generate such a pulse shape.

The reflected wave is produced when the incident wave reaches the specimen and loads it past the elastic limit. In addition, there are other factors that can produce reflections such as an impedance mismatch between components that arises from a change in cross sectional area or material properties. The reflected wave becomes a left-going wave with the opposite sign compared to the incident wave. This wave propagation is illustrated through the use of an x-t wave diagram in Fig 2.1.

The transmitted wave results from the incident wave passing through and loading the specimen. The transmitted wave pulse represents the torque that the specimen experiences. Within the specimen, several reflections build up as the longer incident pulse passes through and interacts with the interface at the end of the specimen. These interactions lead to the specimen experiencing a total torque that is approximated as double the transmitted torque. When the incident torque is much larger than the torque required for yielding the specimen, a large reflected wave and smaller transmitted wave are produced. The maximum magnitude of the transmitted wave is limited by the torque carrying capacity of the specimen.

2.2-1 Strain Measurements

The strain waves in the torsional Kolsky bars are measured by electrical-resistance strain gages. These gages should be oriented at ± 45° with respect to the axial direction of the bar in order to measure the tensile and compressive strains that arise in these directions as a result of the torque. There can be one or two sets of gages on the incident bar and another set on the output bar. Each set of gages is wired in a Wheatstone bridge arrangement consisting of one, two, or four gages. The number of gages used may be selected based on the sensitivity required for the applied torque and material configuration. (Gilat ASM 2000)

Once the loading bar has been clamped and torqued, the clamp is released, allowing the stored strain to propagate through the bar. The initial stored torque wave splits into a left going and right going wave each with half the initial amplitude. Upon reaching the loading wheel, the torsional impedance is large enough to appear as a fixed boundary and reflect the left going wave into a right going wave of equal magnitude. The result is a right going torsional pulse with twice the length of the loading segment and half the initial amplitude. The duration of this pulse is the length of the pulse divided by the shear wave speed of the bar. As the wave passes through the bar, the region underneath the wave experiences a strain equal to the pulse amplitude and all other regions are unloaded and experience zero torque. (Gilat ASM 2000)

It is important to select the locations of the strain gage sets in order to capture a full sample of the incident, reflected, and transmitted waves without overlap. When using a single set of gages on the incident bar, they should be placed at a distance at least twice the loading bar length away from the end of the bar where the specimen is attached. This

ensures that the full incident wave will pass through the gage prior to the arrival of the reflected wave at the gage. Similarly, the gages on the output bar should be placed at a distance at least twice the loading bar length away from the free end of the bar. Once again, this allows the full transmitted wave to pass through the gage before the reflection from the free end arrives. An additional consideration for the output gages is to place the set at least six inches away from the specimen connection on each bar. This prevents additional distortion produced by reflections at the coupling of the specimen.

2.3 Design issues

2.3-1 Transmission and Reflection Coefficients

In linear elastic wave propagation, an incident wave will be split into a transmitted and reflected wave at an interface between two components. The magnitudes of the resulting transmitted and reflected waves are determined by the transmission and reflection coefficient respectively. These coefficients depend on the mass density, shear wave speed and polar moment of inertia of the two components. The derivation of these coefficients from the wave equation is presented.

Along the interface between two elements of different materials and cross sectional area, the continuity conditions are as follows:

$$T_1(0^-, t) = T_2(0^+, t)$$
$$\dot{\theta}_1(0^-, t) = \dot{\theta}_2(0^+, t) \qquad (2.11)$$

The torque and angular velocity are continuous on both sides of the interface. The torque in the material is defined as the rate of twist times the polar moment of inertia and shear modulus.

$$T = GJ\frac{\partial\theta}{\partial x} \tag{2.12}$$

The rate of twist can be related to the angular velocity through the inverse of the shear wave speed.

$$T = GJ\frac{\partial\theta}{\partial x} = GJ(-\frac{1}{c_s}\left(\frac{\partial\theta}{\partial t}\right)) = -\rho c_s J\dot{\theta} \tag{2.13}$$

The torque in the first material is a superposition of the incident and reflected torque waves whereas the torque in the second material is the transmitted torque wave.

.

The polar moments of inertia for a solid circular cross section and ring cross section are defined as follows:

$$J = \frac{\pi}{32}d^4$$
$$J = \frac{\pi}{32}(d_o^4 - d_i^4) \tag{2.14}$$

Substituting the rate of twist definition into the torque definition yields:

$$\dot{\theta}_1 = -\frac{1}{\rho_1 c_1 I_{p1}}(T_i - T_r)$$
$$\dot{\theta}_2 = -\frac{1}{\rho_2 c_2 I_{p2}}T_t \tag{2.15}$$

The impedance for each material is defined as the density time the shear wave speed times the polar moment of inertia.

$$Z_1 = \rho_1 c_1 J_1$$
$$Z_2 = \rho_2 c_2 J_2 \qquad (2.16)$$

Applying these definitions to the original continuity conditions Eq. (2.11) and performing some algebra leads to a definition of the reflected torque coefficient in terms of the impedance of the two materials and the incident torque.

$$T_r = \frac{Z_2 - Z_1}{Z_1 + Z_2} T_i \qquad (2.17)$$

From Eq. (2.17), it is clear that the magnitude of the reflected torque wave coefficient, T_r, increases as the difference in impedance between the two materials increases. Similarly, substituting Eq. (2.17) into Eq. (2.16) results in the transmitted torque coefficient:

$$T_t = \frac{2Z_2}{Z_1 + Z_2} T_i \qquad (2.18)$$

This equation demonstrates that the magnitude of the transmitted torque coefficient, T_t, is primarily dependent on the impedance of the second material. From this relationship, it is clear that, in order to maximize the efficiency of transmitting torque into the specimen, the impedance of the specimen should be as close as possible to the impedance of the bar.

2.3-2 Size requirement for yielding

Taking the transmission coefficient and yielding criteria determined above, one can calculate the range of specimen dimensions that will yield under a specified amount of torque stored in the Kolsky bar. A MATLAB script (Appendix B) was written to combine these conditions and display which specimen dimensions met all of the criteria. Sample plots containing the transmitted torque required, transmission coefficients, and

stored torque required for 1100-O aluminum over a range of wall thicknesses are presented in Fig 2.3.

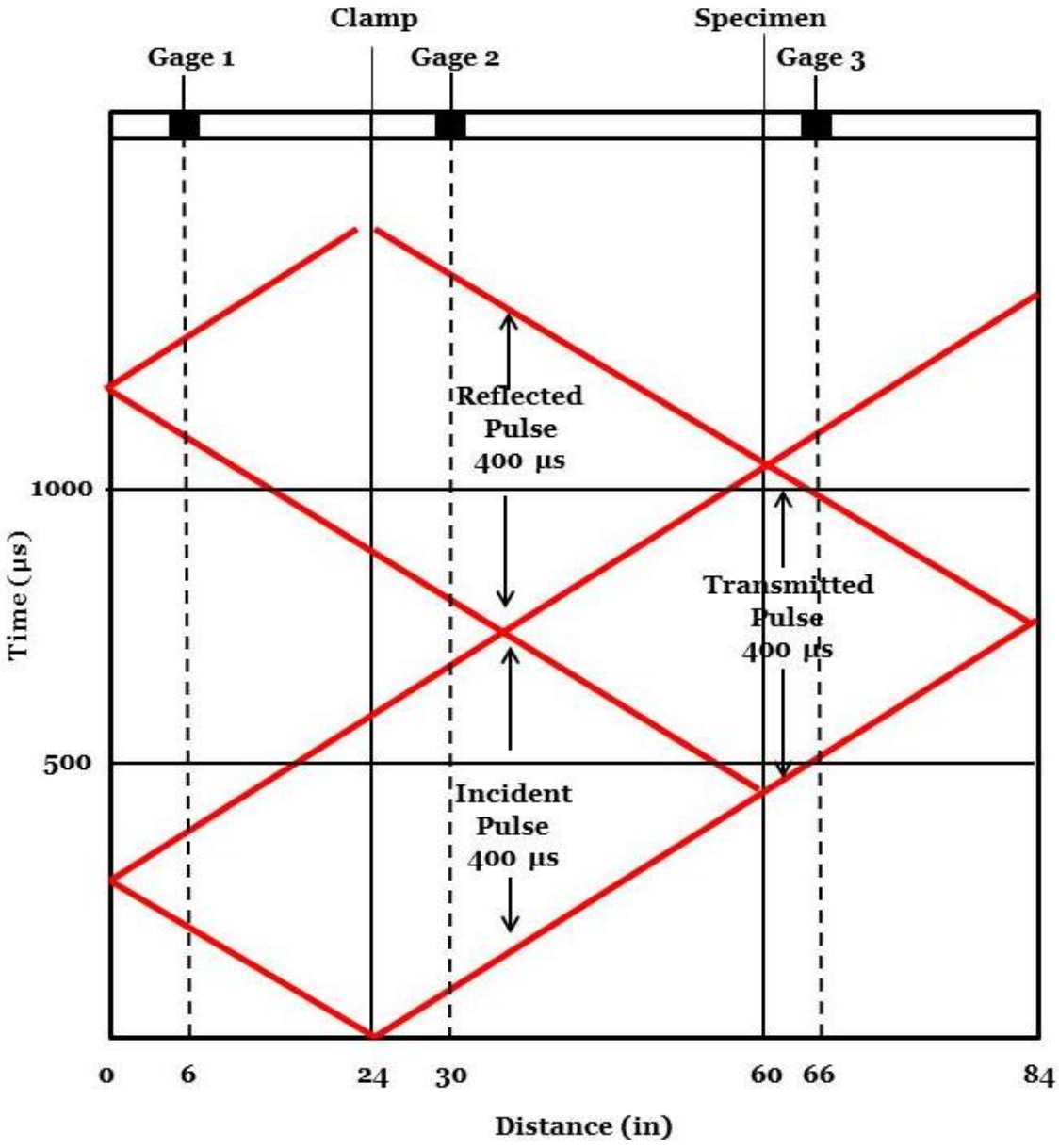

Figure 2.1: Kolsky Bar Schematic overlaid on an x-t diagram

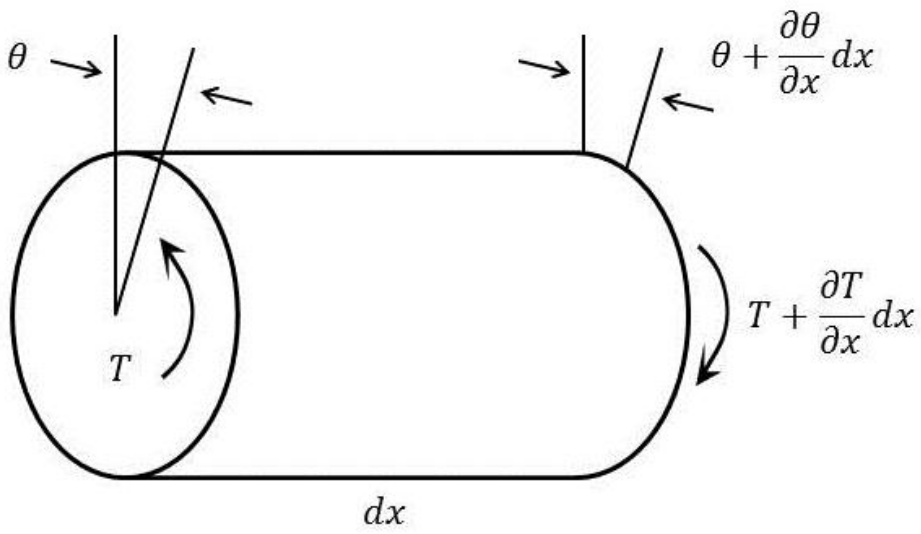

Figure 2.2: Torsional Differential Element

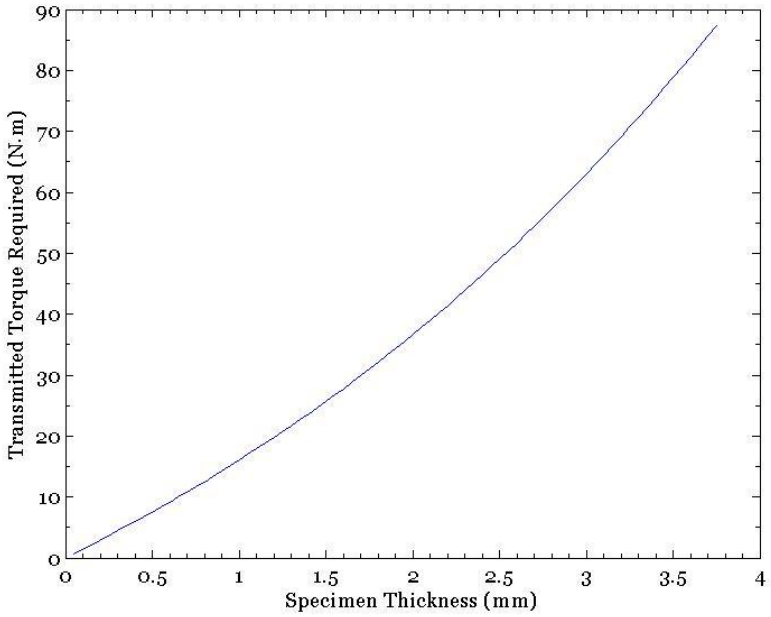

Figure 2.3a: Transmitted torque required to produce a 100 MPa shear stress in an aluminum specimen with a 9.5 mm inner diameter.

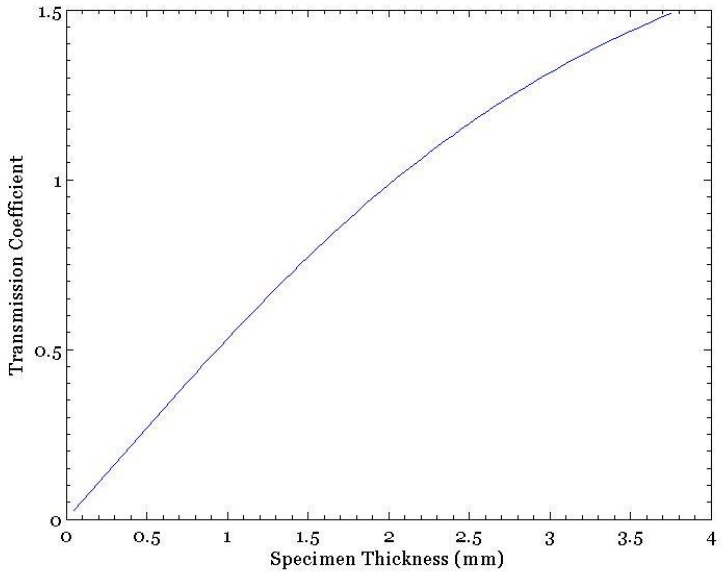

Figure 2.3b: Transmission coefficient between an aluminum rod of diameter 12.7 mm and an aluminum specimen with a 9.5 mm inner diameter.

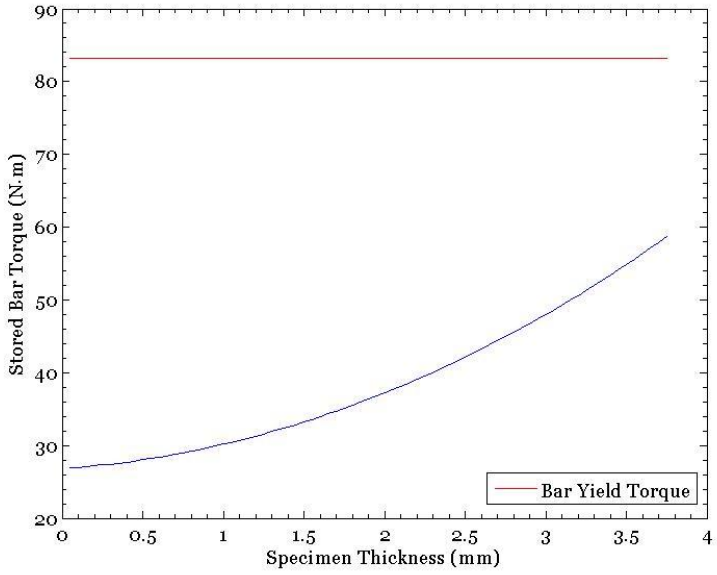

Figure 2.3c: Stored torque required in the input bar to produce a 100 MPa shear stress in an aluminum specimen with a 9.5 mm inner diameter.

Chapter 3: Design and Implementation

The main objective of this thesis was to construct an apparatus for testing specimens in high strain rate torsion. In this chapter, the design, construction, and implementation of the torsional Kolsky bar is described in detail.

3.1 Kolsky Bar Design

This experiment utilizes a conventional torsional Kolsky bar with the addition of a pioneering optical measurement system. The configuration of the Kolsky bar used in this study is largely based on the one described by Gilat (1994) with a custom designed clamping mechanism. The parameters for this bar were determined by first considering the shear yield stresses of the desired specimen materials, 80 MPa for 6061-O aluminum and 60 MPa for 1100-O aluminum.

For the bar to generate large plastic strains in the specimens, it must be able to generate a shear stress significantly greater than the shear yield stress of the material. To be a reusable system, this torque must induce a shear stress well below the yield strength of the loading bar. This sets a minimum value for the diameter and composition of the bar. However, it is also necessary for the prescribed shear stress to produce an easily measurable shear strain to obtain useful information from the experiment. Therefore, the loading bar could not exceed a certain diameter or be made from a material with a very large Young's modulus.

From these requirements, a 12.7 mm diameter 6061-T6 aluminum rod was selected as the loading bar material. Under the desired torque calculated for yielding the specimen in Section *3.1-3*, the shear stress in the bar would be 91 MPa. This shear stress

is well within the shear yield strength of 207 MPa for the bar and produces a shear strain of 3.5 millistrain which is within the measurement range of standard strain gages. The minimum length of the input bar and incident bar is determined by the desired length of the stress wave pulse. In general a longer bar produces a smoother signal than a shorter bar. Due to space limitations, the length of the total system is about 7 feet in contrast to the 12 foot long system described by Gilat. The input bar is 60 inches long with a loading section than can vary between 12 and 24 inches and the output bar is 26 inches long. The final design can be seen in schematic and constructed form in Fig. 3.1.

3.1-1 Clamp, Loading

The key components of a Kolsky bar system are the clamping, loading, and release mechanisms. For loading, this bar uses an 8 inch aluminum loading wheel Fig. A.4 attached to the end of the loading bar that is torqued through a ratcheting pulley system. The clamp is based on the one described by Gilat (2000) but redesigned to fit in a smaller space and is simpler to construct. The clamp consists of two symmetric arms that fit around the half inch loading bar and are supported by a pin attached to a support block anchored to the I-beam foundation as shown in Fig. 3.2. The clamping force is applied through a steel bolt above the loading bar and a hydraulic cylinder acting normal to the side of the clamp below the loading bar as well as the reacting force applied by the side of the structure. The release occurs by continued application of force by the cylinder used to clamp the bar. The bolt holding the clamp is notched so that it fractures abruptly as it is placed in tension by the motion of the hydraulic cylinder. This configuration maintains a symmetric loading from both the cylinder and the normal force from the side wall. This is

crucial to the operation of the system as it does not apply a bending moment to the bar which is a significant source of signal noise.

3.1-2 Fracture Pin

The notched bolt placed above the loading bar is known as the fracture pin and serves as the release mechanism to start a test. The design of the pin is a key component of the system as it determines what the maximum magnitude of the stress pulse as well as the magnitude of the strain rate. The pin must be strong enough to apply friction to the bar to store an adequate amount of torque. In addition, the pin must fracture under the load supplied by the cylinder. This is ensured by notching the pin and applying a pre-torque. The notch size and torque magnitude are two parameters that can be varied to obtain the desired loading condition. An ideal configuration would permit the storing of torque up to the shear yield stress of the bar. The pin configuration selected for this experiment is a medium strength steel rod with nominal diameter of 6.35 mm and a notch diameter of 3.94 mm. Rupture of the pin occurred rapidly, resulting in a release of the torque with a rise time of about 30 μs.

3.1-3 Specimen

The materials to be used in this experiment are 6061-O and 1100-O aluminum machined into thin walled tube specimens. The specimens have a gage length of either 2.54 mm or 12.7 mm and a wall thickness varying between 0.3 and 1.2 mm. Once machined to the specified dimensions, the aluminum specimens appear as shown in Fig. 3.3. The specimens are then painted matte white with red lines drawn across the gage length as seen in Fig. 3.4 for imaging purposes. The two ends of the specimen are

hexagonal flanges that are mated to the input and output bars through matching collars, the implementation of which can be seen in Fig. 3.5. Using linear elastic mechanics of material behavior for a circular section, the transmitted torque required in the loading bar to generate the specified shear stress in a sample specimen was calculated. For an 1100-O aluminum sample with an inner diameter of 9.5 mm and outer diameter of 11.5 mm, the transmitted torque required to reach the shear yield stress of 62 MPa is 10 N·m.

A key factor in linear elastic wave propagation is the transmission coefficient at an interface between two components described in detail in Chapter 2. Taking the transmission coefficient into account, a stored torque required in the loading bar was calculated. For the same specimen configuration as presented above, to produce a transmitted torque of 10 N·m a stored torque of 19 N·m is required. This analysis also includes the torque multiplying effect within the specimen and the double stored torque magnitude. A general MATLAB code was written to calculate the stored torque required for a desired shear stress in a specimen of any dimension and material.

3.1-4 Instrumentation

There are three sets of strain gages placed along the bar, as shown in Fig. 3.1a, to measure the initial strain, incident and reflected waves, and the transmitted wave. All of the strain gages used are Micro Measurements 062TH-ST-EA-120 gages with gage factor: 2.0, resistance: 120 Ω. The first set of strain gages measuring the initial strain stored in the loading bar is located 6 inches from the loading wheel and connected in a Wheatstone quarter-bridge configuration. The first set of gages are used primarily as a triggering mechanism for the oscilloscope and therefore do not require accuracy beyond

what the quarter-bridge configuration offers. The second set of strain gages measuring the incident and reflected waves is located 54 inches from the loading wheel and connected in a Wheatstone half-bridge configuration. The third set of strain gages measuring the transmitted wave is located 20 inches from the free end and connected in a Wheatstone half-bridge configuration. The second and third sets of gages are recording the relevant wave data and therefore require the greater accuracy and stability supplied by the half-bridge configuration. Vishay 2210A Signal Conditioning Amplifiers are used to excite the strain gages and to output the amplified voltage to a Tektronix Oscilloscope.

The strain gages were attached to the bar using the recommended procedures. The surface of the bar was abraded with sandpaper and excess material was cleaned with acetone. The surface was prepped first using the neutralizer solution which was allowed to dry before applying the conditioner. The catalyst solution was then applied to both the surface of the bar and the strain gage. M-Bond adhesive was then applied to the surface of the bar whereupon the strain gage was placed under pressure and heat for several minutes. Once the adhesive cured, wires were soldered on the contact leads to connect the strain gage to the signal conditioning amplifier. Due to the small size of the gages and the diameter of the bar, the strain gages may not have been placed exactly along the principal torque axis. The direction of the gage placement is known to within ± 2° which would correspond to an error of ± 7% in the measurement of the maximum strain at any of the gage stations.

3.1-5 Construction

To build the torsional Koslky bar, a drawing of each of the components was first made in SolidWorks™ and can be seen in Appendix A. The experimental apparatus is supported by a platform consisting of an I-beam and three vertical supports. The steel I-beam section was purchased; its surface was made flat by grinding and then the set of holes shown in Fig A.1 were drilled. The three supports were constructed from rectangular steel tubing. The loading wheel, bar supports, input, and output bars were all machined from aluminum and assembled as shown in Fig. 3.1. The bar supports were mated to the I-beam through bolt connections at roughly 18 inch intervals. The bar supported containing the clamping system could be placed at three different locations depending on the length of the loading pulse required.

3.2 High-speed camera and cone mirror imaging

In addition to the strain gages, this experiment introduced an optical measurement system consisting of a conical mirror and high speed camera as shown in Fig. 3.6. The conical mirror is made from a steel plate that is machined to have an inverted conical surface and polished to be highly reflective. The mirror is arranged behind the specimen to reflect the entire surface of the cylindrical specimen into the camera at the end of the supporting beam. The mirror and camera were carefully aligned to capture an undistorted image of the specimen. Additional lighting is required to facilitate the capture of high speed imagery so four lamps were arranged around the specimen in the configuration shown in Fig. 3.6. A Photron SA1 camera was connected to a computer for recording the

images and to the oscilloscope for triggering.

The captured images then underwent an unwrapping procedure to extract the undistorted surface of the specimen for analysis. A general schematic of the imaging geometry and mapping from the wrapped to the unwrapped state is shown in Fig. 3.7. Following the procedure described in (Zhang et al., 2010), points *V (p,q)* from the initial circular image are mapped to points *M (m,n)* in the rectangular processed image. This is accomplished using the following relationships:

$$p = p_0 - r\sin\theta$$
$$q = q_0 - r\cos\theta \tag{3.1}$$

where r and θ are defined as:

$$r = r_i + h\left(\frac{w-m}{w}\right)$$
$$\theta = 2\pi\left(\frac{n}{u}\right) \tag{3.2}$$

The quantities u and w correspond to the length and width of the unwrapped image and are determined by:

$$u = 2\pi r_s$$
$$w = h/\sin(2\pi - 2\alpha) \tag{3.3}$$

where $\alpha = 65°$ for the cone mirror, r_s is the specimen radius in the initial wrapped image and h is the width of the specimen circular band in the wrapped image. This process is automated through the use of a MATLAB script (Appendix B) to unwrap all of the captured images. The primary source of error in this process is introduced by a misalignment between the conical mirror and the camera. This causes the wrapped

images to be distorted by not uniformly distributing the circumference of the specimen on the surface of the mirror.

3.3 Preliminary Calibration

Once the torsional Kolsky bar was constructed, a preliminary calibration was conducted to confirm its operation and reveal characteristic signal artifacts in the system. These signal artifacts are reflections produced by elements in the bar system other than the specimen and will be present in all measurements. Identifying these artifacts allows for their removal from recorded specimen data and results in more accurate calculations of stress and strain.

3.3-1 Isolated Input Bar

The behavior of the input bar was investigated by isolating it from the output bar. This system simply consists of the stored torque region and the rest of the input bar with the two sets of strain gages monitoring the strain response of the bar. The test was conducted by first applying the clamp and loading the stored torque region of the bar. The clamp was then broken, releasing the torque. The resulting incident and reflected waves are shown in Fig. 3.8. The shape of the two waves is roughly the same and the peak amplitudes match. The reflected wave has a longer rise time and the steady portion of the pulse has an approximately 15% lower magnitude than the incident pulse. Some of this behavior can be attributed to dissipation of the torque in the rod. However, this discrepancy is primarily a result of the collar at the end of the input bar. The collar has a larger diameter than the input bar and transitions from a solid bar to a hollow section. These effects will need to be taken into consideration when analyzing specimen data.

3.3-2 Solid Coupling

To examine the behavior of the output bar and transmitted wave, a solid coupling test was performed. The solid coupling test involves connecting the input and output bars together with an object with impedance that matches the two bars. Ideally, this results in the entire incident wave being transmitted and no reflected wave. The results from this test are presented in Fig. 3.9. The expected transmitted wave is defined as the difference between the incident and reflected waves. The transmitted wave exhibited a similar rise time and reached a lower steady amplitude than the incident wave. The average magnitude of the transmitted wave was about 10% lower than the incident wave. This result can mostly be attributed to the collars mating the coupling piece to the bars whose summed cross-sectional area was not identical to the input and output bars. The other effect of this mismatch is seen in the non-zero reflected wave which drops to a negative value shortly after the initial peak of the wave.

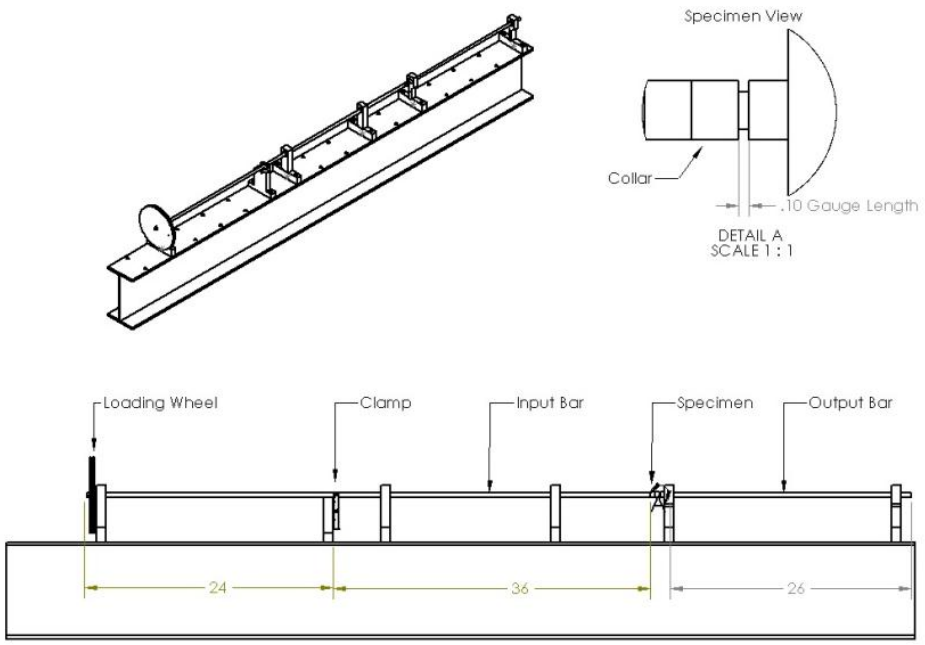

Figure 3.1a: Torsional Kolsky Bar Assembly Diagram

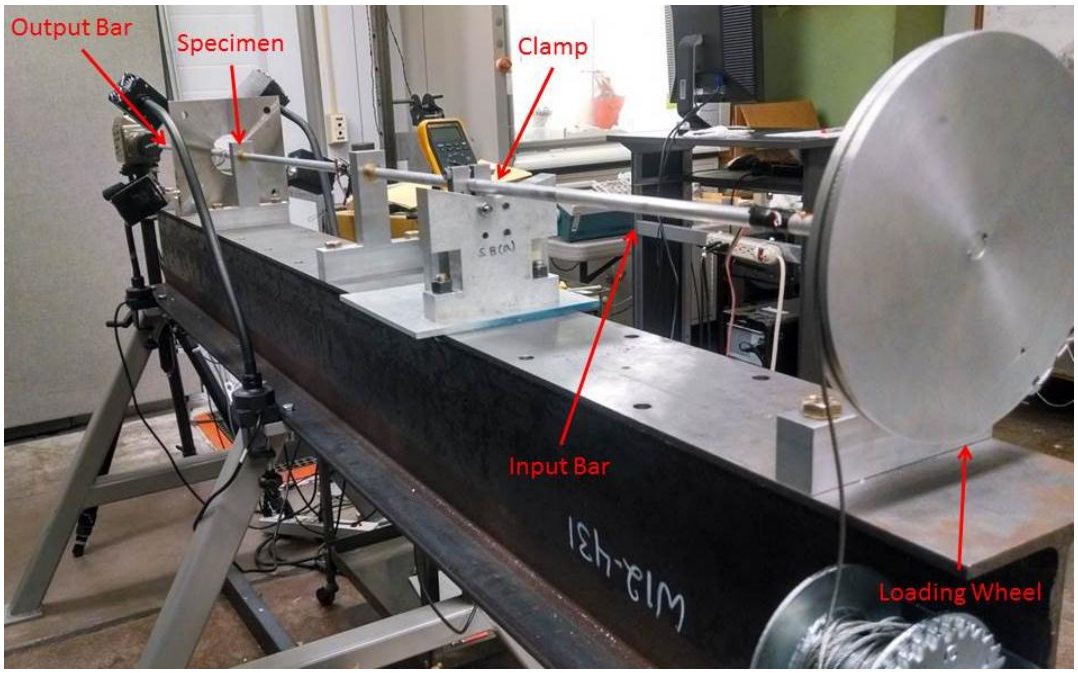

Figure 3.1b: Torsional Kolsky Bar Assembly

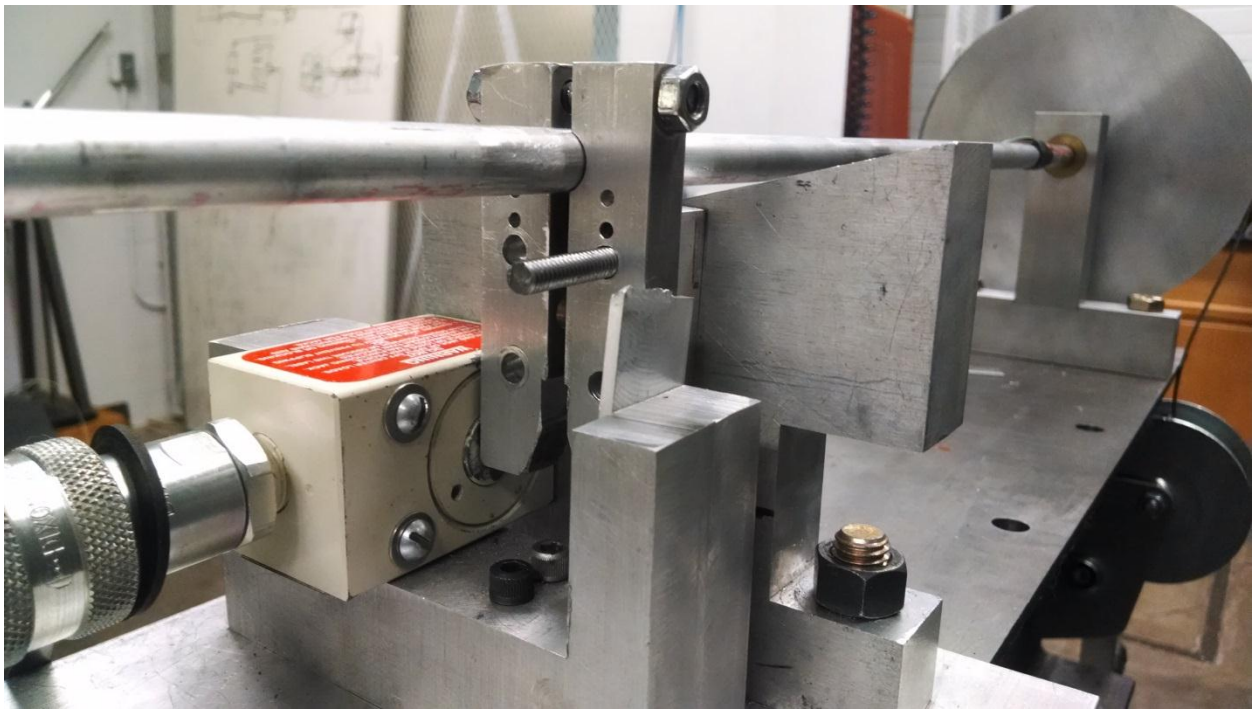

Figure 3.2: Clamp Assembly

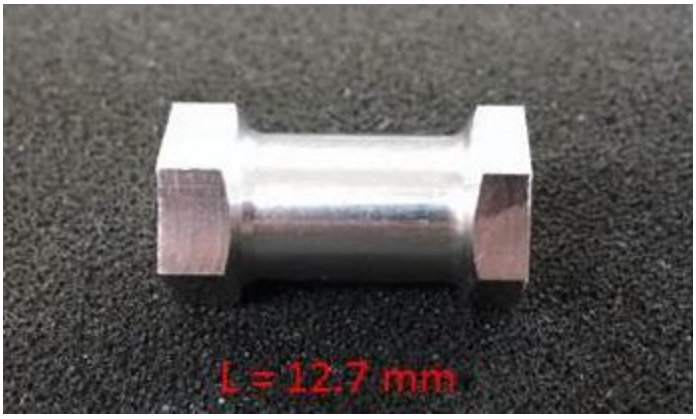

Figure 3.3: Aluminum Specimen

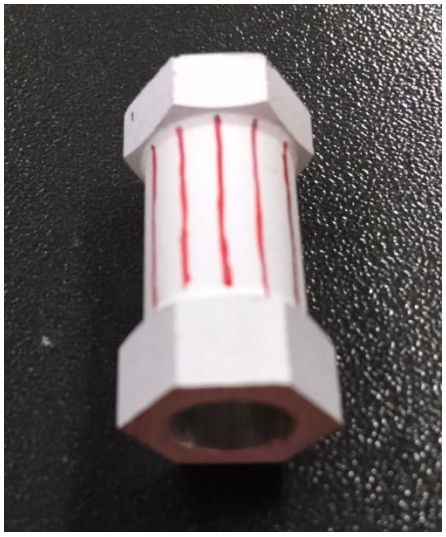

Figure 3.4: Painted Aluminum Specimen

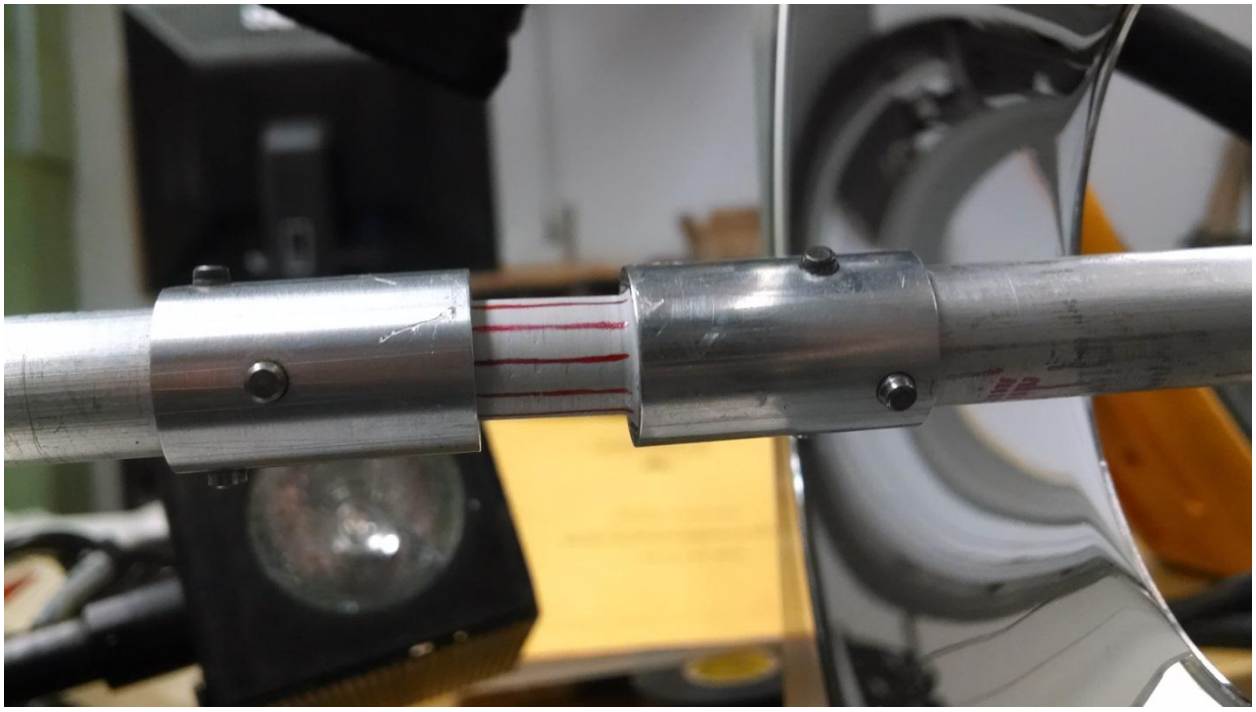

Figure 3.5: Specimen Arrangement

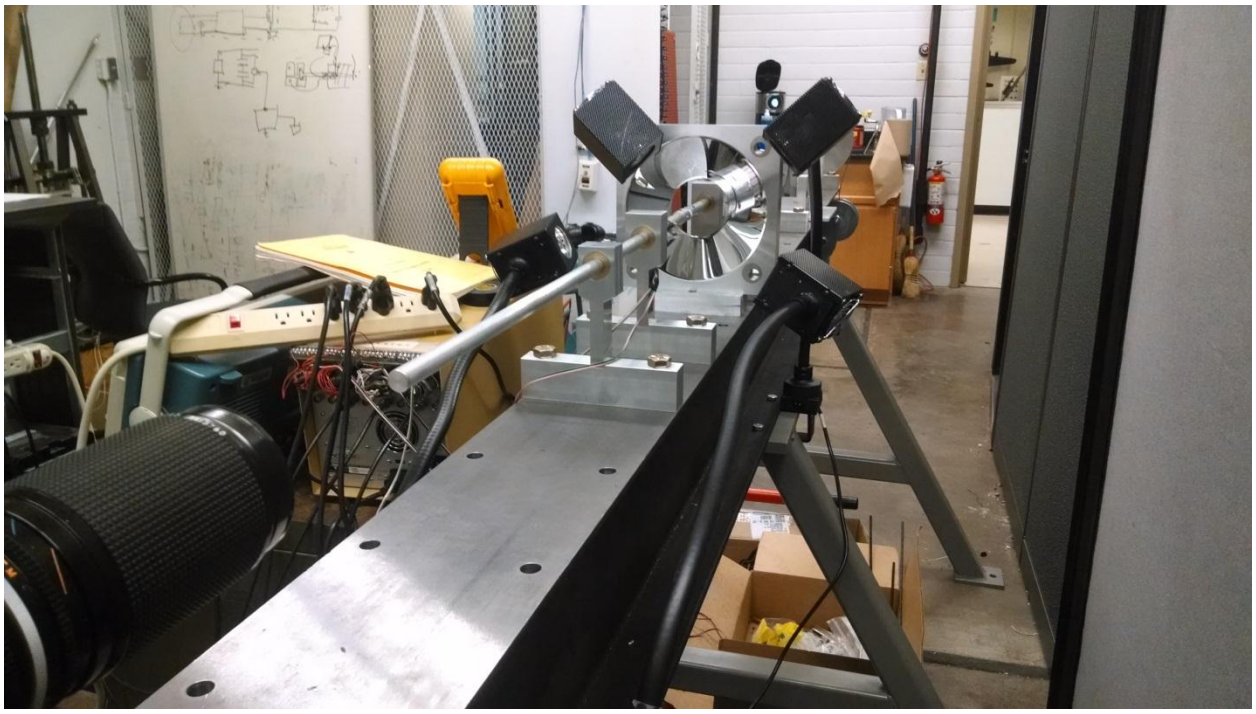

Figure 3.6: Photron Camera and Cone Mirror Arrangement

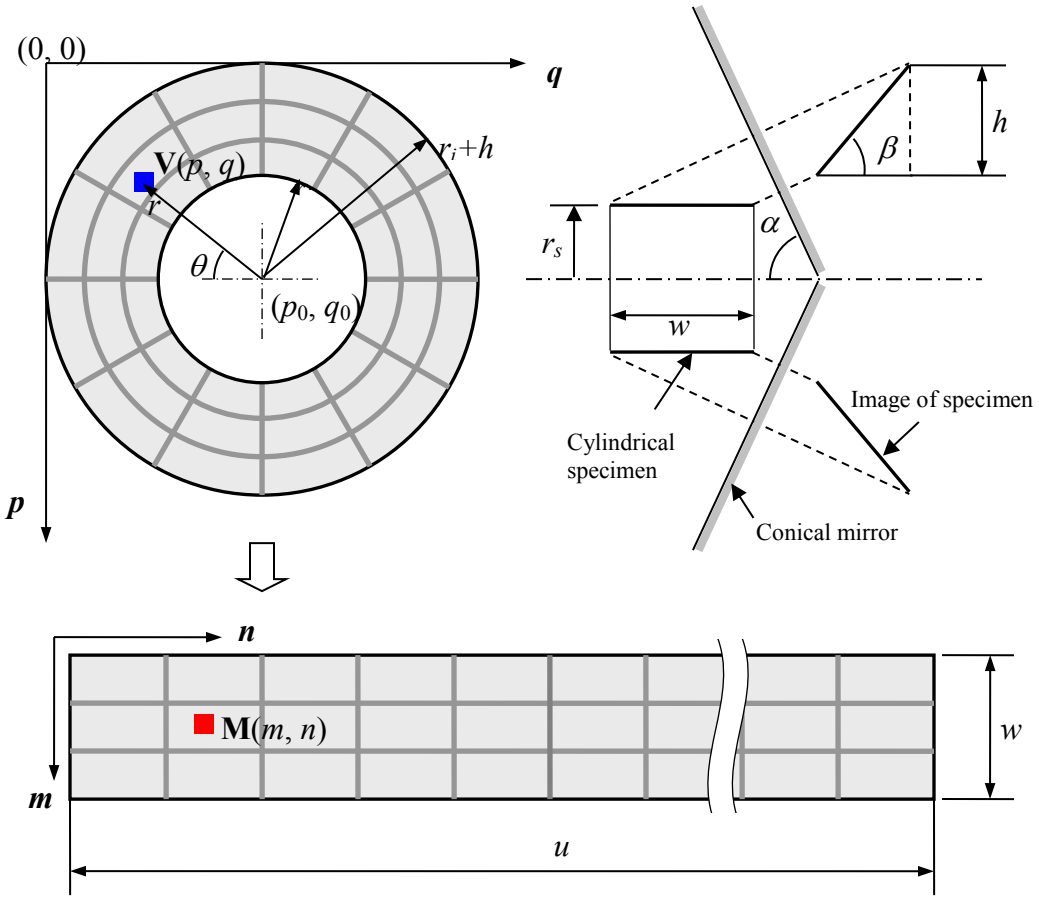

Figure 3.7: A schematic diagram showing the imaging optics for the conical mirror and procedure to map the image projected on the conical mirror to the developed image of the surface of a cylindrical specimen. (Zhang 2010)

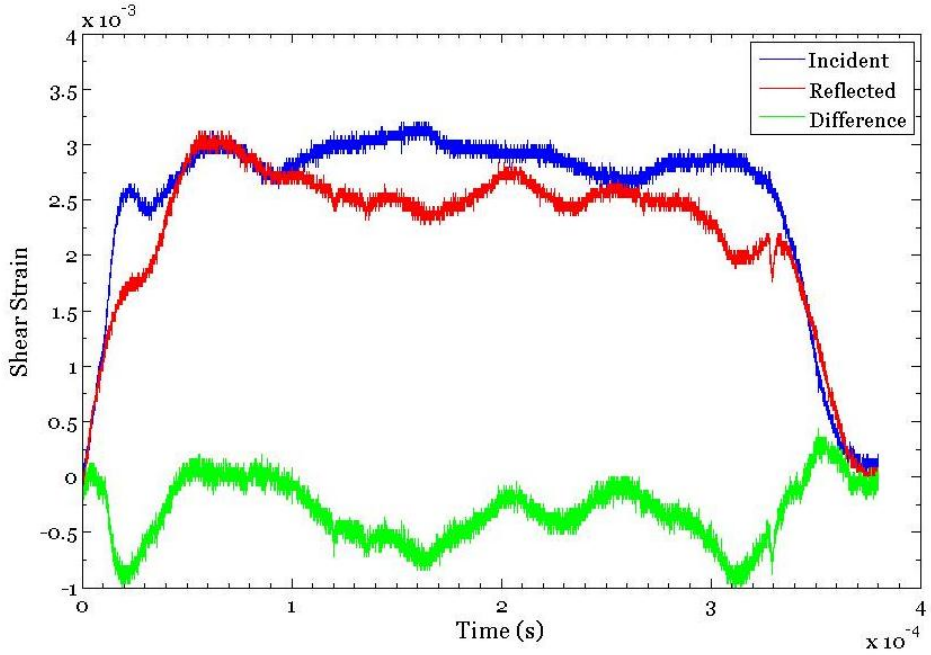

Figure 3.8: Isolated Input Bar

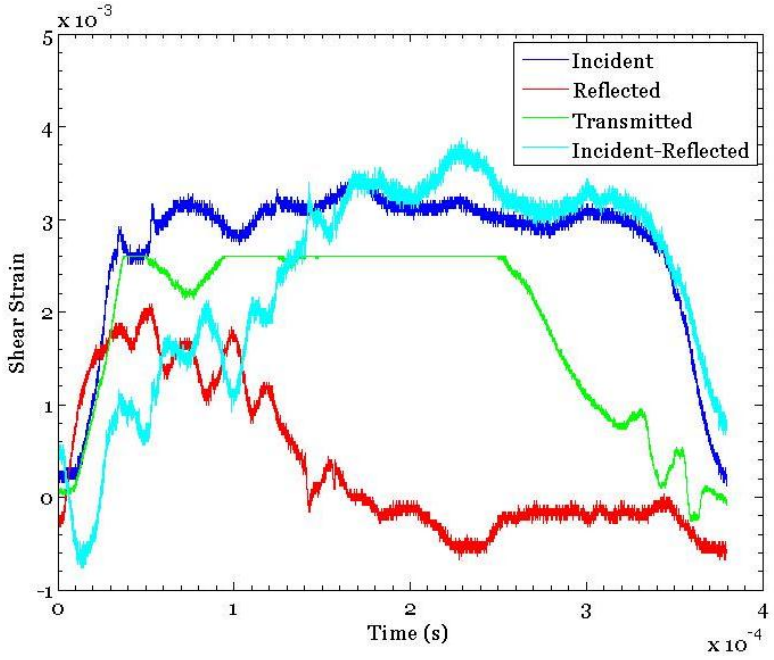

Figure 3.9: Solid Coupling Test

Chapter 4: Experiments

This chapter describes the specimens, the data analysis process, and the events contained in a typical experiment. The specimen description consists of the materials used and the fabrication process. The experiment section describes the procedure as well as the data and results from a typical test performed on each specimen material. The post-processing section entails a torsional wave analysis and optical strain measurement analysis. The final section presents and examines the results from the analysis.

4.1 Specimen Materials and Fabrication

Aluminum specimens were utilized in this experiment to minimize the impedance mismatch with the aluminum Kolsky bar and for their relatively low shear yield strength as compared to steel. Two aluminum alloys were studied: 6061-O and 1100-O. These annealed alloys were used because they possess the lowest shear yield strength and exhibit higher strains than the heat-treated alloys.

4.1-1 6061-O Aluminum Specimens

The first set of experiments was conducted with specimens made of 6061-O aluminum. The main alloying elements of 6061 aluminum are magnesium and silicon. Magnesium comprises 0.8-1.2% and silicon comprises 0.4-0.8% weight percent of the alloy. The Kolsky bars are made from the heat treated variant of this alloy and overall it is one of the most commonly used aluminum alloys. The relevant material properties for

this experiment are the shear modulus $G = 26$ MPa, density $\rho = 2.7\ \mathrm{g/cm^3}$, and shear yield strength $\tau_Y = 82.7$ MPa.

Starting with stock hexagonal Aluminum 6061-T6 tubes, the specimens were machined into short thin walled tubes with hexagonal flanges. The desired inner diameter was obtained by drilling and reaming the appropriately sized through hole on the lathe. The required gage length and outer diameter were then produced using the side cutting tool also on the lathe. Once the desired specimen geometry was made, the aluminum 6061-T6 specimens were subjected to an annealing procedure to remove the heat treatment and produce aluminum 6061-O specimens. The annealing procedure consisted of the following:

- The 6061-T6 aluminum specimens are placed in the furnace
- The furnace is heated to a temperature of 760° F
- The temperature is held at 760° F for two hours
- The furnace is then cooled by 50° F every hour down to 500° F
- The furnace is then turned off and the specimens are allowed to cool to room temperature overnight in the furnace.

The purpose of the annealing procedure is to make the material more ductile and to lower the shear strength.

4.1-2 1100-O Aluminum Specimens

The second set of experiments was conducted with specimens made of 1100-O aluminum. The 1100 alloy contains greater than 99% weight percent aluminum and only

trace amounts of alloying elements of which silicon and iron are the most prevalent at less than 0.95% weight percent. The density and shear modulus for this material are the same as for 6061-O aluminum but the shear yield strength $\tau_Y = 62.1$ MPa.

Starting with the stock round Aluminum 1100-O rods, the specimens were machined into short thin walled tubes with hexagonal flanges. The hexagonal flanges were first machined on the mill using a hexagonal collet to obtain the correct geometry between faces. The desired inner diameter was obtained by drilling the appropriate sized through hole on the lathe. The required gage length and outer diameter were then produced using the side cutting tool also on the lathe. This material was notably more difficult to machine due to its high ductility, resulting in peeling instead of cutting the material under normal conditions. This was mitigated through the liberal use of coolant and avoiding fine cuts under ten thousandths of an inch.

4.2 Torsional Kolsky Bar Experiment

This section will describe the events contained in the experiment and present a summary of the collected raw data. There were five tests conducted with 6061-O aluminum specimens with a gage length of 12.7 mm and wall thickness varying between 0.25 and 1.5 mm. In addition there were seven tests conducted with 1100-O aluminum specimens, five of which possessed a gage length of 12.7 mm and wall thicknesses between 0.5 and 0.8 mm. The remaining two specimens had a gage length of 2.5 mm and a wall thickness of 0.5 mm. A range of specimen dimensions were used to observe how the strain rate experienced by the specimen varied with wall thickness.

4.2-1 Experiment Procedure

Prior to conducting the experiment, the instrumentation was initialized. First, the strain gage amplifier and oscilloscope were turned on. By adjusting the gain, the strain gages were calibrated so that an output of 1 volt corresponded to 1 milli-strain. The excitation signal for the strain gages was engaged and once the gages reached a steady temperature, they were balanced. The Photron camera and software were set to capture the images at 30,000 frames per second which corresponds to one frame per 333 micro seconds. The four lamps that illuminate the specimen were also turned on at this stage. The oscilloscope was set such that it recorded 1 millisecond of data after it was triggered by the voltage of the stored torque gage dropping upon the release of the clamp.

After the instrumentation was been set, the clamp was engaged and the fracture pin was torqued using a torque wrench to 90 in·lbs. The hydraulic cylinder was then loaded to 1200 psi to complete the clamping of the loading bar. The loading wheel was then turned to apply the desired torque which was monitored through the strain gage on the loading bar. A typical test was conducted at a torque of approximately 40 N·m which was recorded as 4 millistrain by the strain gage. This has been established as the practical limit for this system as higher torques delaminate the strain gages when released. Once the desired torque has been applied, the hydraulic cylinder loaded the clamp to take the fracture pin to failure.

4.2-2 Raw Data

The unprocessed results from both a 6061-O and 1100-O aluminum specimen test are presented in this section. The 6061-O test was performed with a specimen of gage

length 12.7 mm and wall thickness 1.5 mm. The incident torque recorded by the strain gage was 40.1 N·m. The resulting strain waves are shown in Fig. 4.1 plotted against time. The blue line is the stored strain recorded by the first set of strain gages and is initially at 8 milli-strain but the magnitude quickly drops to 4 milli-strain as the pulse splits into left and right going waves. The recorded strain then drops to zero as the wave propagates down the bar beyond the stored strain region. The red line corresponds to the second set of strain gages which records the incident and reflected waves. The green line is the strain recorded by the third set of strain gages on the output bar and corresponds to the transmitted wave. The incident, reflected and transmitted waves are displayed in more detail in Fig. 4.2. There is a noticeable amount of noise in the isolated signals that generates an uncertainty of ± 0.125 milli-strain in the strain measurement at any given time. There is some error in the identification of the start time for each strain wave due to the noise level in the signals that may be as large as 20 μs. This variability in the start time will lead to some errors in the early stress and strain calculations but will be negligible in the later steady-state calculations.

A sample set of images recorded by the Photron camera of the specimen reflected on the surface of the cone mirror are available in Fig. 4.3. From these images, it is clear when the wave is transmitted through the specimen as the initially radial lines begin to twist. Once the wave has passed through, the lines remain in place until the reflection comes and unloads the specimen.

4.3 Post-processing and Analysis

4.3-1 Torsional Kolsky Bar Analysis

The method employed to determine the shear strain and shear stress from the data collected by the strain gages mounted on the torsional Kolsky bar is well documented in the ASM Handbook (Gilat 2000) and proceeds as follows.

For a homogeneous state of stress in the specimen, the strain in the transmitted bar equals the difference of the incident and reflected strains.

$$\gamma_T = \gamma_I + \gamma_R \tag{4.1}$$

The strain rate is obtained as:

$$\dot{\gamma}_s = \frac{2cD_s}{L_s D}\gamma_R(t) \tag{4.2}$$

The total shear strain in the specimen can be obtained by integrating the strain rate over the duration of the wave pulse:

$$\gamma_s = \frac{2cD_s}{L_s D}\int_0^t \gamma_R(t)dt \tag{4.3}$$

The average torque in the specimen is defined as the mean of the torques at the near and far end of the specimen.

Therefore, the shear stress in the specimen to be found as:

$$\tau_s = \frac{GD^3}{8}\frac{\gamma_T(t)}{D_s^2 t_s} \tag{4.4}$$

The shear strain and shear stress in the specimen are then calculated by applying formulas (4.3) and (4.4) to the recorded reflected and transmitted waves. A MATLAB

script available in Appendix B was written to automate the processing of the raw strain gage data into stress and strain values for the specimens.

4.3-2 Image Analysis

After an experiment was conducted, the images recorded during the test were saved using the Phantom camera software. These images were then processed using the unwrapping MATLAB script described in Chapter 3. For each test there were approximately twelve images which corresponded to the initial stress wave passing through the specimen. These unwrapped images were then processed using another MATLAB script, available in Appendix B, in which the user traces the path of the vertical lines drawn on the specimen. As the specimen is strained, the lines turn and the relative angle between the initial vertical line and the line in the current frame corresponds to the angle of twist on the surface of the specimen.

4.4 Dynamic Torsion Test Results

4.4-1 6061-O Aluminum Results

For this analysis, a sample 6061-O aluminum specimen of gage length 12.7 mm, outer diameter 10.9 mm, and wall thickness 1.5 mm is used. In this test, the loading bar was torqued to strain of 8 milli-strain measured by Gage 1 in Fig 4.1 which corresponds to a stored torque of 80.3 N·m. Once the clamped was released, the stored wave propagated as an incident wave with a magnitude of 4 milli-strain as seen in Fig 4.2a. The resulting reflected and transmitted waves shown in Fig. 4.2b, 4.2c had a mean magnitude

of approximately 2.4 milli-strain and 1 milli-strain respectively. The relative magnitudes of the incident and transmitted strains indicate that the specimen had a transmission coefficient of 0.25. The reflected wave is implemented in Eq. (4.2) to calculate the strain rate, the result of which is presented in Fig 4.4a. The specimen experienced a peak strain rate of 1480 s^{-1} which is typical for a torsional Kolsky bar. The strain rate was integrated using Eq. (4.3) to calculate the shear strain displayed in Fig. 4.4b. The resulting curve is linear with rounded edges. Eq. (4.4) was applied to the transmitted wave to obtain the shear stress presented in Fig. 4.4c. The calculated shear stress and shear strain were combined to produce the curve presented in Fig 4.5, showing the strain hardening behavior of the material. The true stress and true strain are obtained from the measured shear stress and shear strain through the following operations.

$$\sigma = \sqrt{3}\tau_s(1+\epsilon)$$
$$\epsilon = \ln(1+\frac{\gamma_s}{\sqrt{3}}) \qquad (4.5)$$

The expected true stress – true strain curve produced by the Ramberg-Osgood model is described by:

$$\sigma = \sigma_Y(1+\beta\epsilon_P)^n \qquad (4.6)$$

where σ_Y is the yield stress, ϵ_P is the plastic strain, β and n are numerical parameters. For 6061-O aluminum, the yield stress is 25 MPa, β is 14165, and n is 0.22. A comparison between the measured values and Ramberg-Osgood fit for true stress and true strain is presented in Fig 4.6. Outside of the initial offset, the measured values correlate well to the calculated curve demonstrating the effectiveness of the torsional Kolsky bar and the accompanying analysis. The expected shear localization is not observed because

the specimen did not reach high enough strains. This can be rectified by lengthening the pulse by extending the loading bar or by shortening the specimen. The current configuration of the bar does not allow for the loading bar to be extended beyond 18 inches. The alternative is to shorten the specimen which would negate the addition of the optical system as the specimen would no longer be visible.

A series of the unwrapped images is displayed in Fig. 4.7 and shows the progression of torsional pulse as the lines twist at a constant rate with respect to the initial orientation. The blue line is the referenced position and the red line is the current position of the line. This angle of twist can be converted to shear strain through the use of a geometric conversion factor. The necessity of this factor arises from the distortion in the ratio between the radius and length of the specimen present in the cone mirror images. A comparison of the shear strains calculated from these images and the strains calculated using the torsional Kolsky bar analysis is displayed in Fig. 4.8. The image derived strains correlate well with the wave analysis strains despite the coarseness and variability of the image strains. This coarseness results from the relatively large time step of approximately 33 microseconds between images. The primary source of the variability in the image strain measurement is the user defined start and end points of each line as well as the limited number of pixels in the source images.

4.4-2 1100-O Aluminum Results

Sample data from an 1100-O aluminum specimen of gage length 12.7 mm, outer diameter 10.9 mm, and wall thickness 0.7 mm is presented in this section. This test was conducted with a stored torque of 80.3 N·m as measured by Gage 1 in Fig. 4.9. The

incident, reflected, and transmitted waves are presented in Fig 4.10. The relative magnitude of the transmitted wave compared to the incident wave corresponds to a 0.25 transmission coefficient. The strain rate experienced by the specimen Fig. 4.11a is calculated from the reflected wave using Eq. (4.2) and has a maximum value of 1250 s^{-1}. The strain rate is integrated by applying Eq (4.3) to determine the shear strain over time Fig. 4.11b. The 1100-O specimen shear strain exhibits a similar shape as the 6061-O specimen shear strain with a slightly different slope as determined by the strain rate. The shear stress is calculated from the transmitted strain by applying Eq. (4.4), producing Fig. 4.11c. Combining the calculated values produces the shear stress – shear strain plot in Fig. 4.12. Examining this plot reveals a peak stress of 97 MPa at a shear strain of five percent followed by a dip in the stress before the stress reaches a steady state around 87 MPa.

A comparison is made between the stress response of two specimens with a 12.7 mm gage length and a specimen with a 2.5 mm gage length in Fig. 4.13. The two longer specimens have wall thickness of 0.7 mm and 0.8 mm corresponding to average strain rates of 922 s^{-1} and 972 s^{-1}. There is a small but noticeable difference in the rise time and peak stress at the two strain rates. The elastic behavior of the material cannot be reliably determined from this analysis because the stress in the specimen does not reach equilibrium due to the high rate of loading. The short specimen has a wall thickness of 0.5 mm and a much larger strain rate of 5029 s^{-1}. The 1100-O specimen exhibits a large change in response due to the higher strain rate, demonstrating significant strain rate dependence.

The images recorded during the experiment by the camera in Fig 4.14 are converted to the set of unwrapped images in Fig. 4.15. These images reveal the response of the material to the torsional stress wave pulse. The initial axial translation is a result of the hexagonal flange slipping in the collar before it engages and the specimen is torqued. The rate of change in the angle of twist seen in these images is converted to the shear strain through a geometric scaling factor and compared to the shear strain calculated using wave analysis in Fig. 4.16.

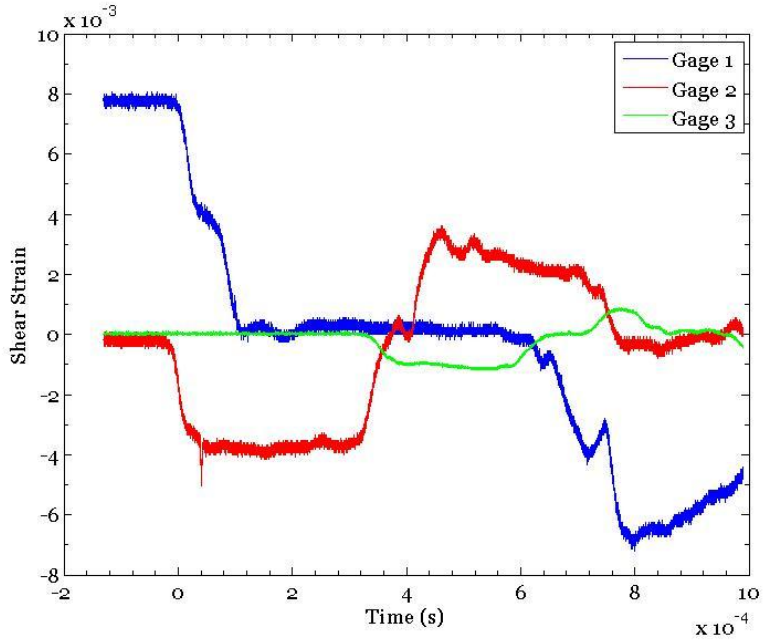

Figure 4.1: 6061-O Aluminum Strain Gage Measurements

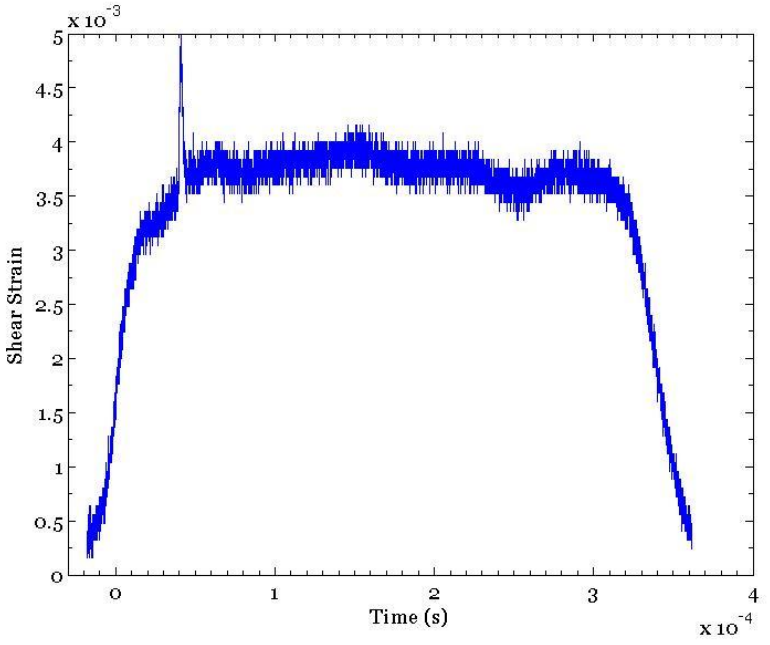

Figure 4.2a: 6061-O Aluminum Incident Wave

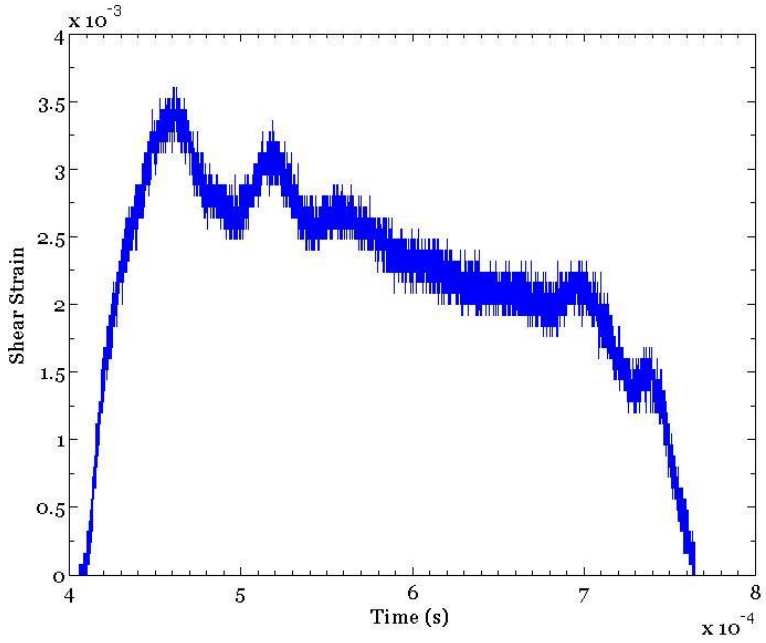

Figure 4.2b: 6061-O Aluminum Reflected Wave

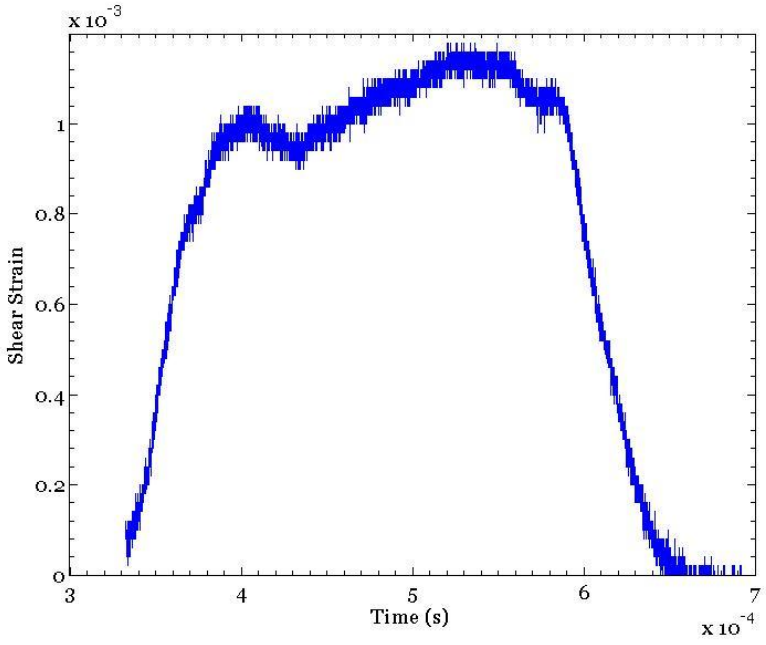

Figure 4.2c: 6061-O Aluminum Transmitted Wave

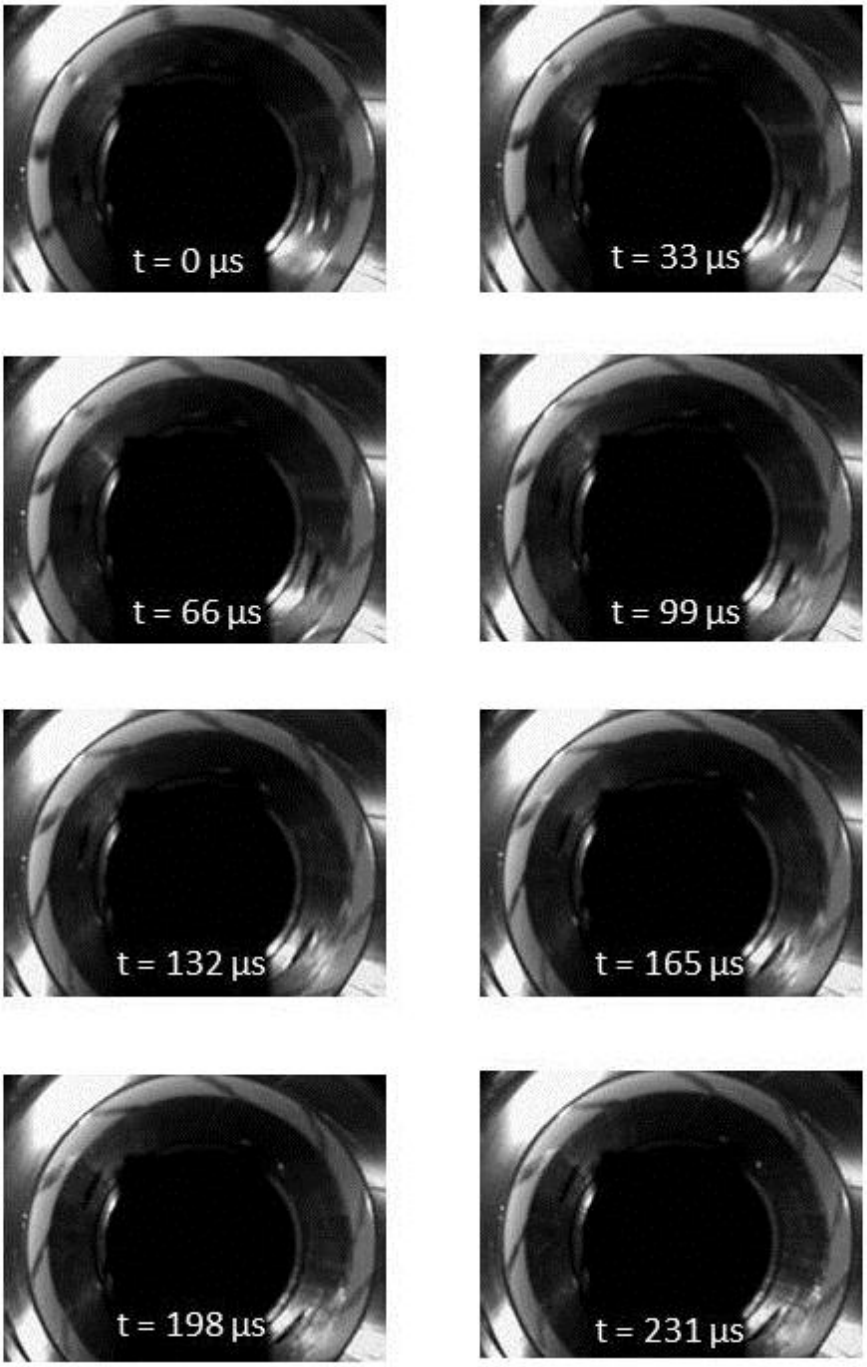

Figure 4.3: 6061-O Aluminum Photron Images

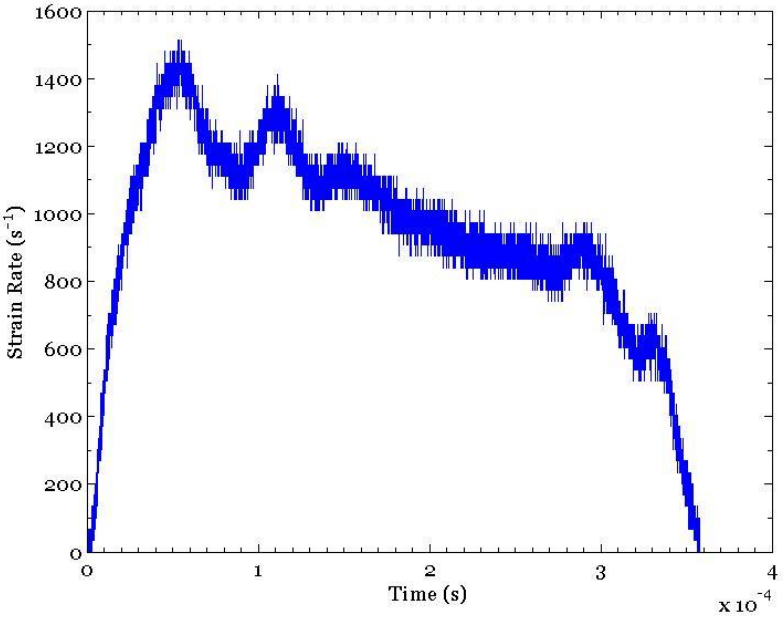

Figure 4.4a: 6061-O Aluminum Strain Rate

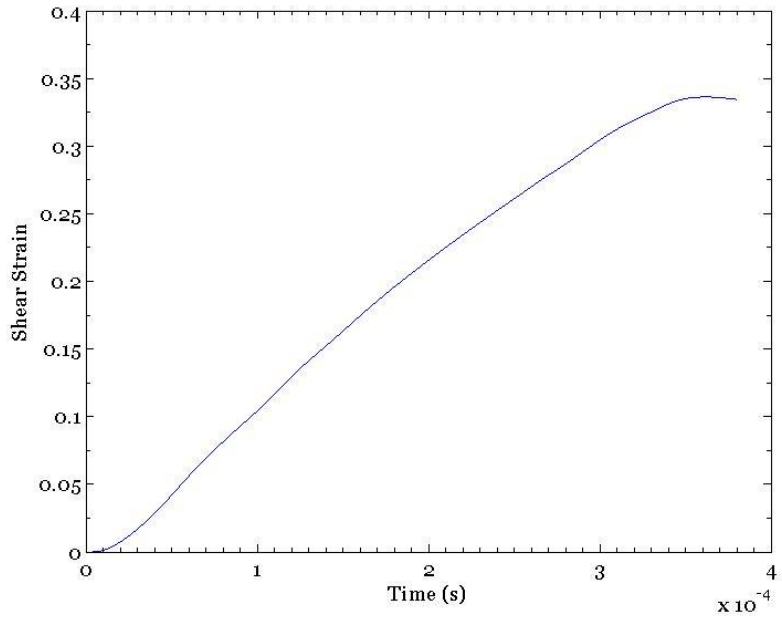

Figure 4.4b: 6061-O Aluminum Shear Strain

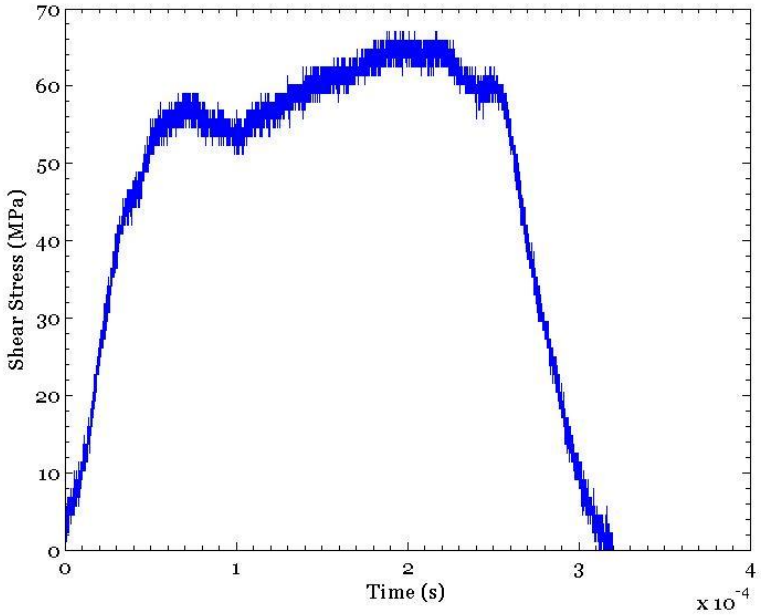

Figure 4.4c: 6061-O Aluminum Shear Stress

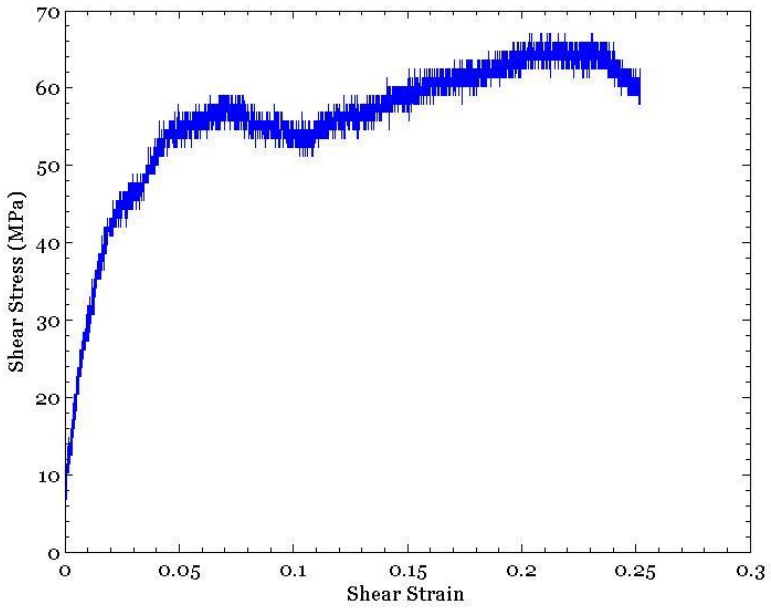

Figure 4.5: 6061-O Aluminum Shear Stress – Shear Strain Curve

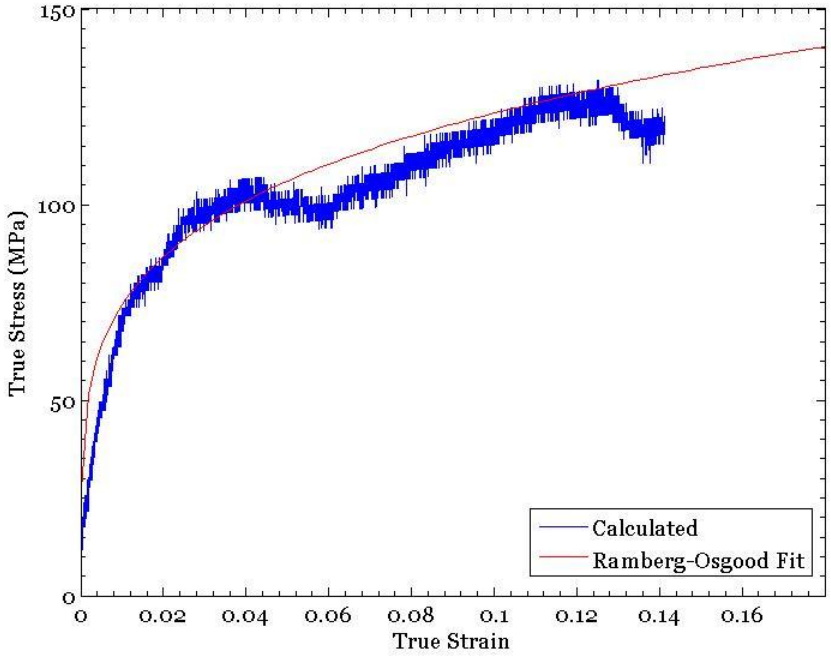

Figure 4.6: 6061-O Aluminum Ramberg-Osgood fit comparison

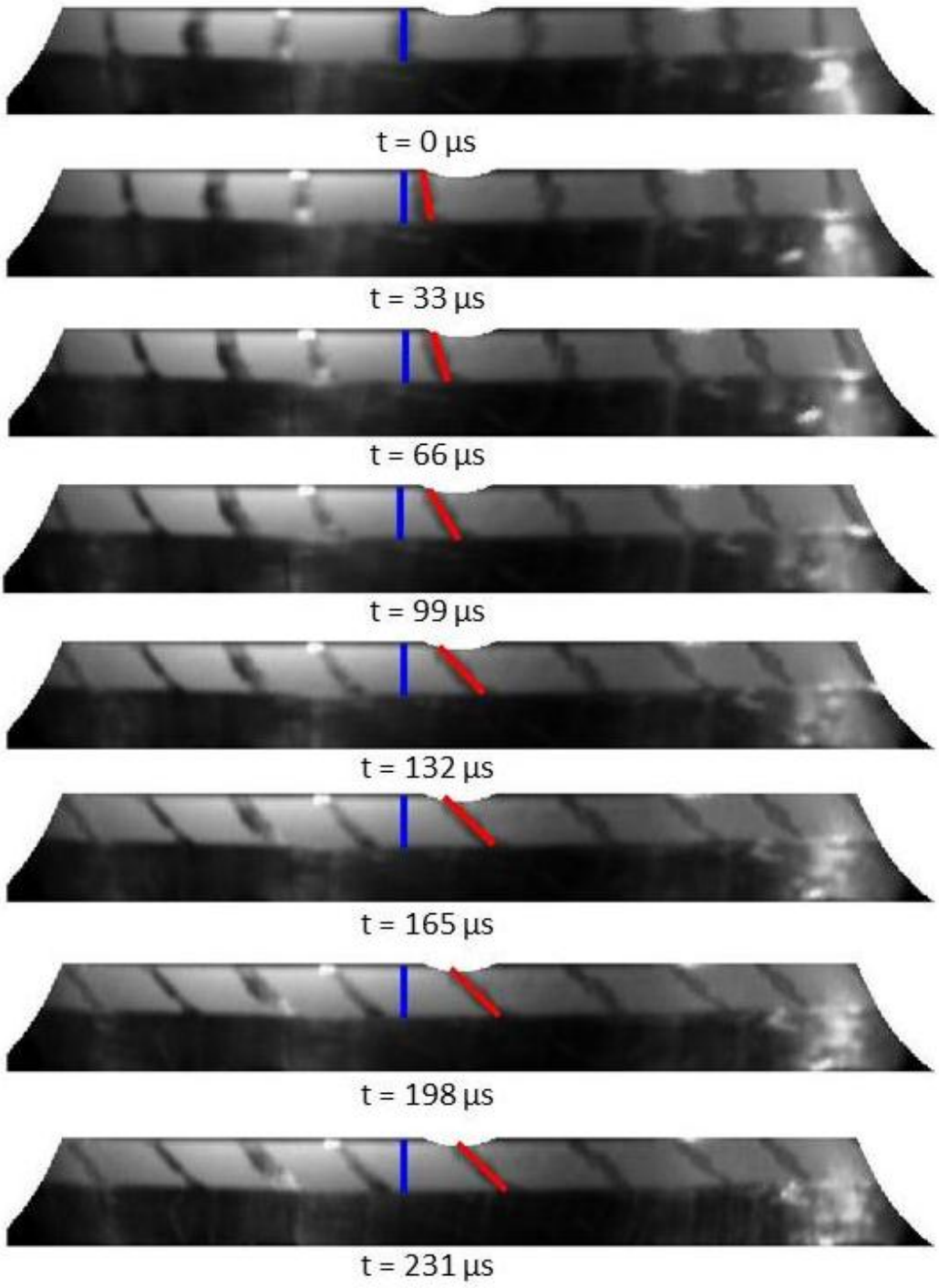

Figure 4.7: 6061-O Aluminum Unwrapped Images

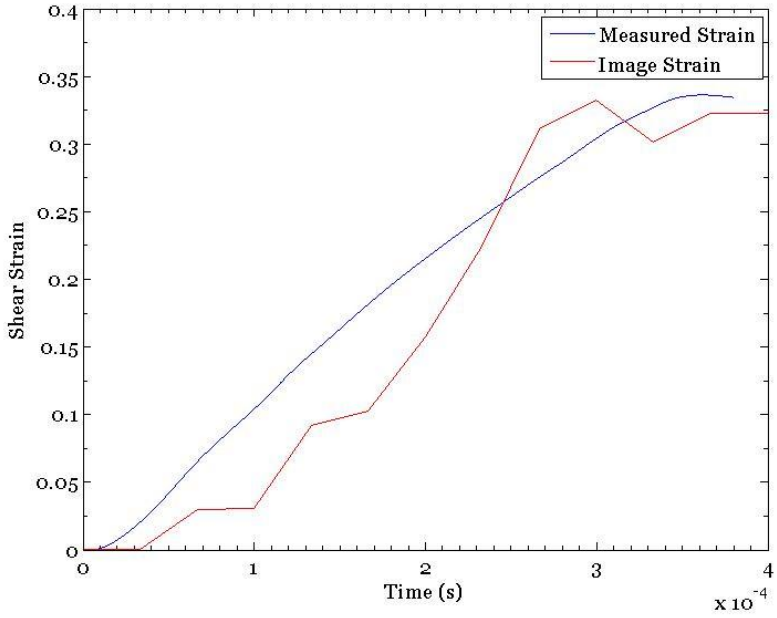

Figure 4.8: 6061-O Aluminum Strain Measurement Comparison

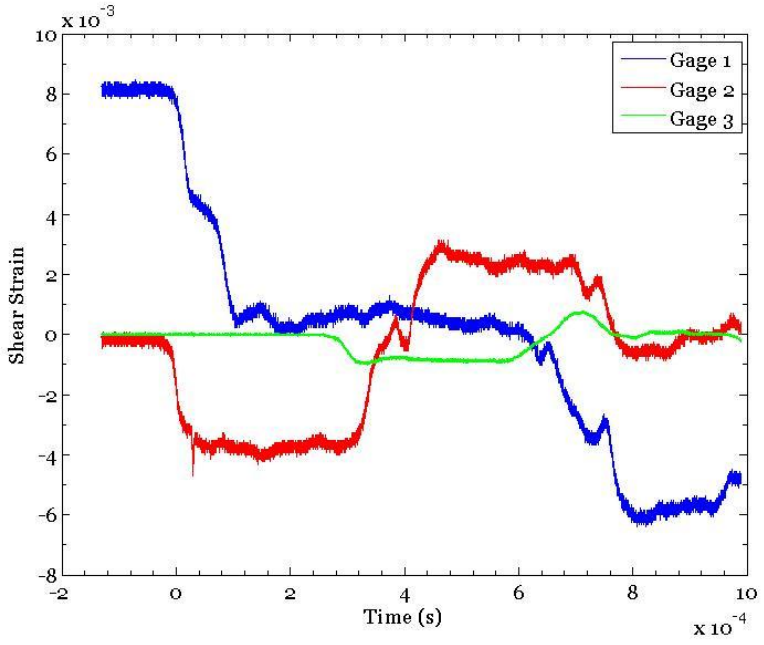

Figure 4.9: 1100-O Aluminum Strain Gage Measurements

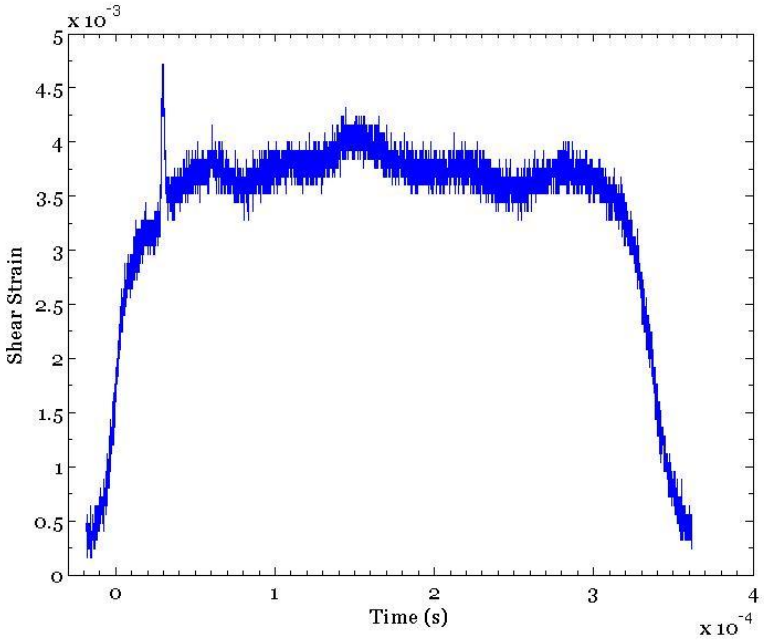

Figure 4.10a: 1100-O Aluminum Incident Wave

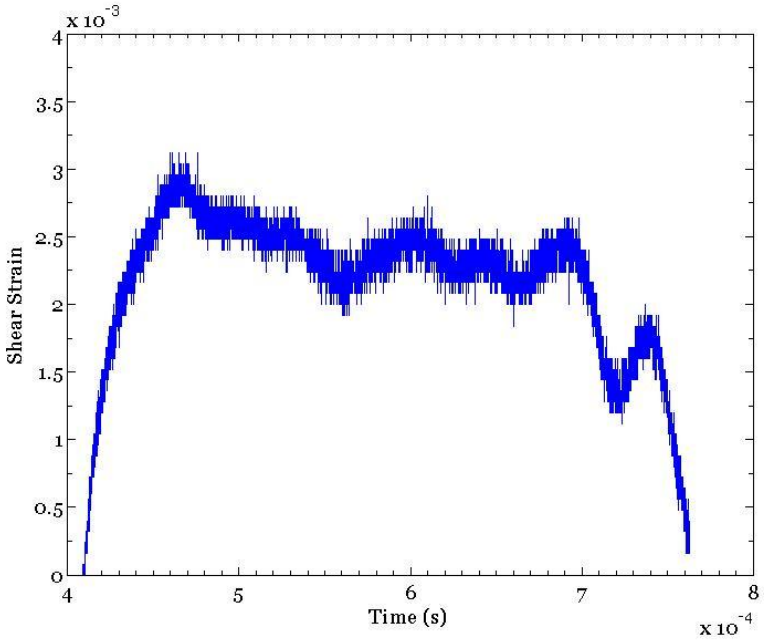

Figure 4.10b: 1100-O Aluminum Reflected Wave

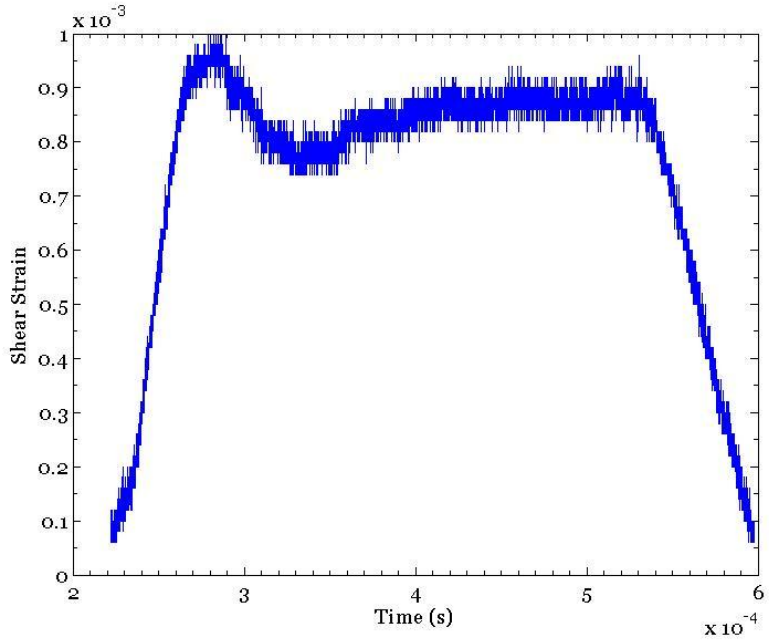

Figure 4.10c: 1100-O Aluminum Transmitted Wave

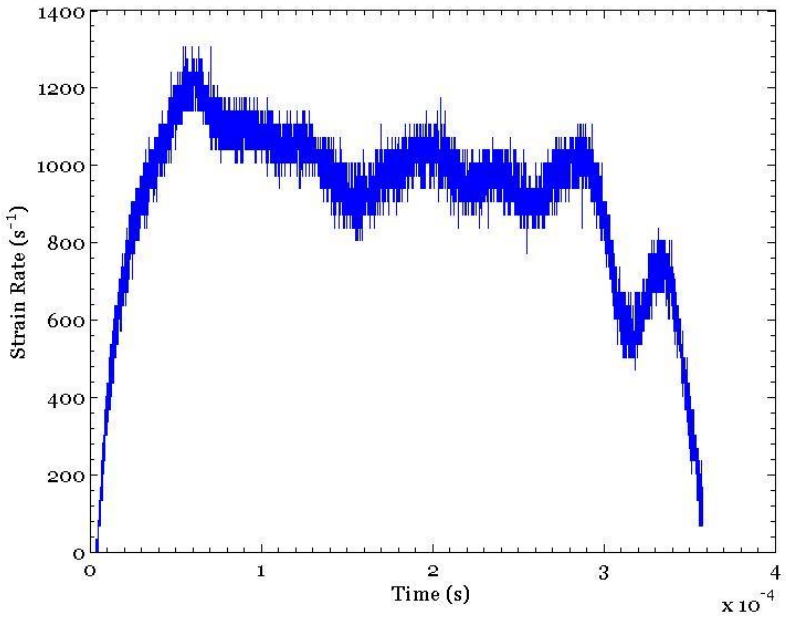

Figure 4.11a: 1100-O Aluminum Strain Rate

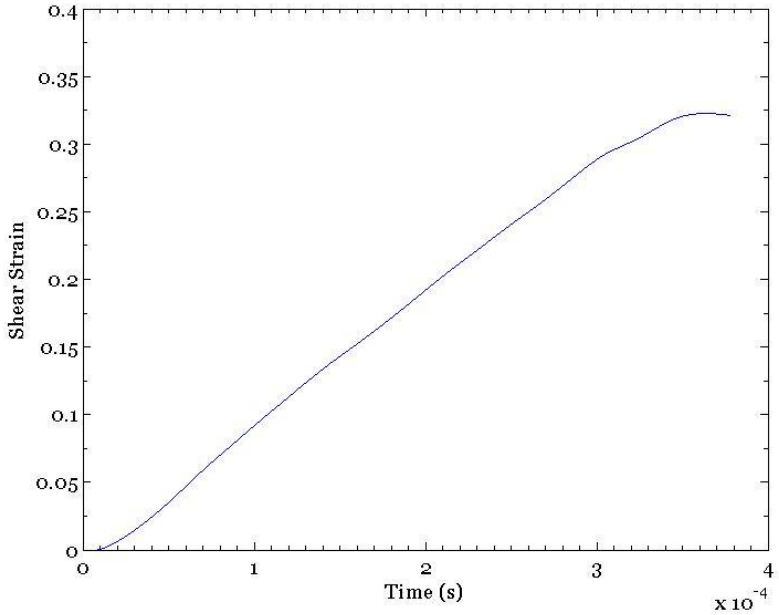

Figure 4.11b: 1100-O Aluminum Shear Strain

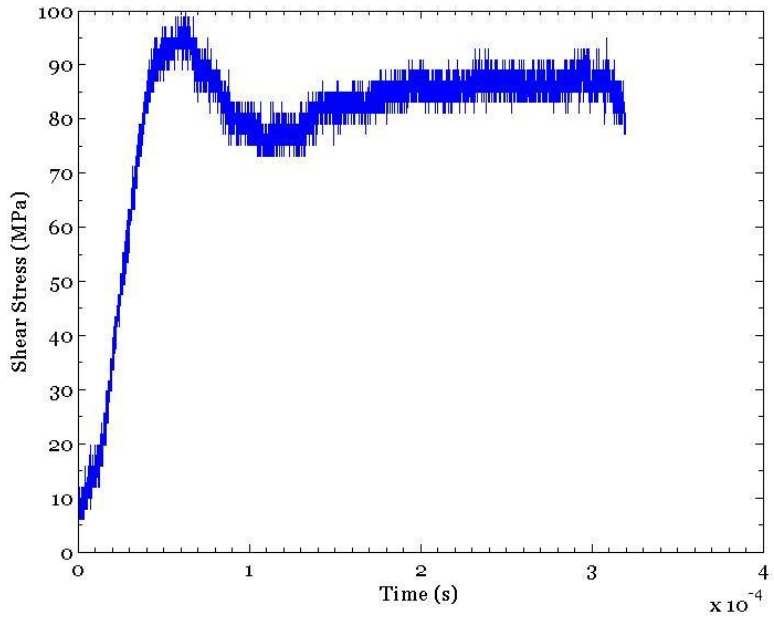

Figure 4.11c: 1100-O Aluminum Shear Stress

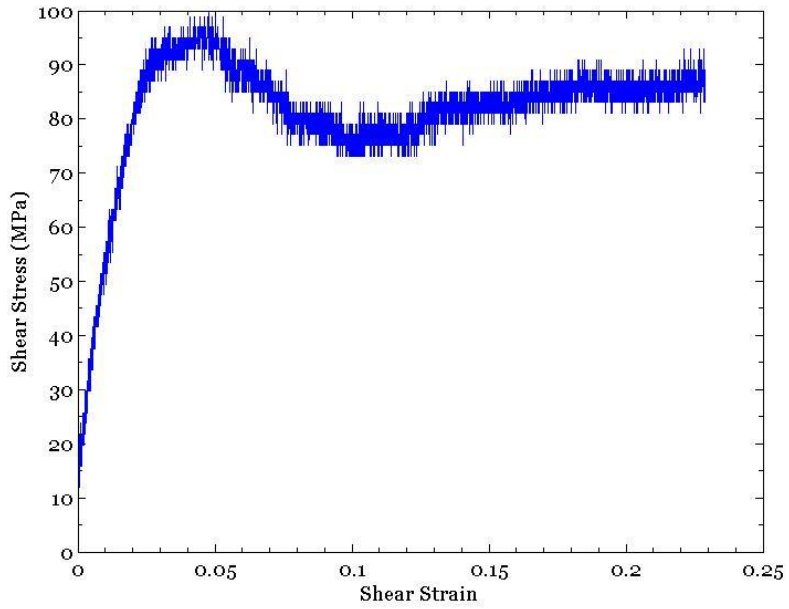

Figure 4.12: 1100-O Aluminum Shear Stress – Shear Strain Curve

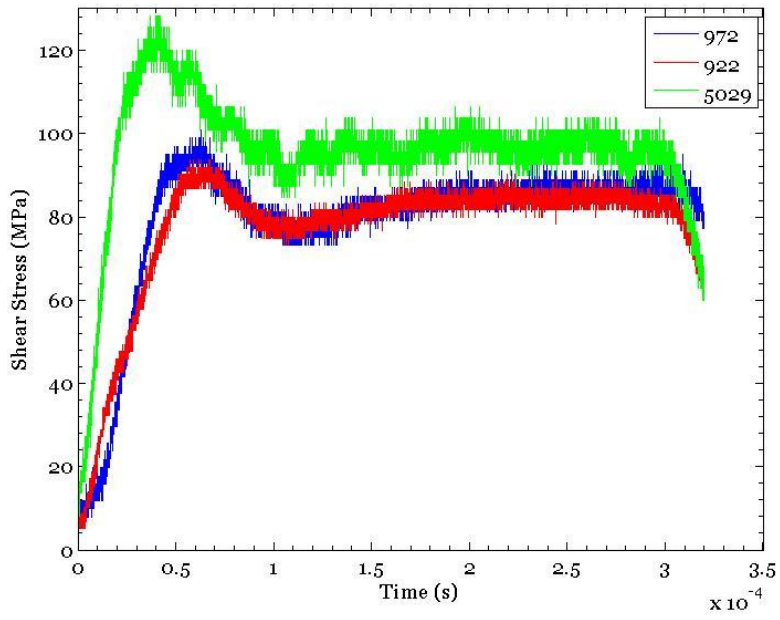

Figure 4.13: 1100-O Aluminum Strain Rate Dependence

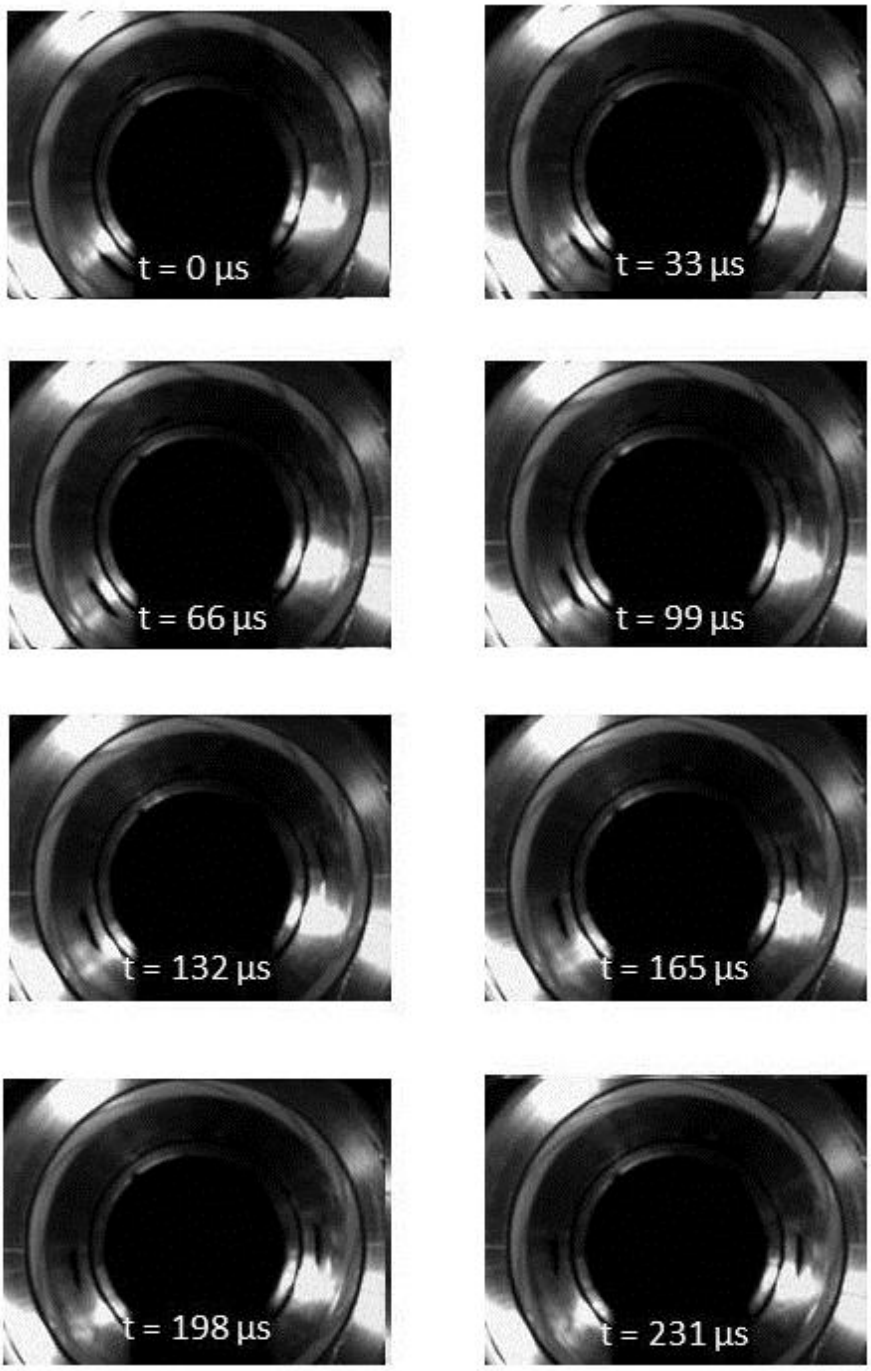

Figure 4.14: 1100-O Aluminum Photron Images

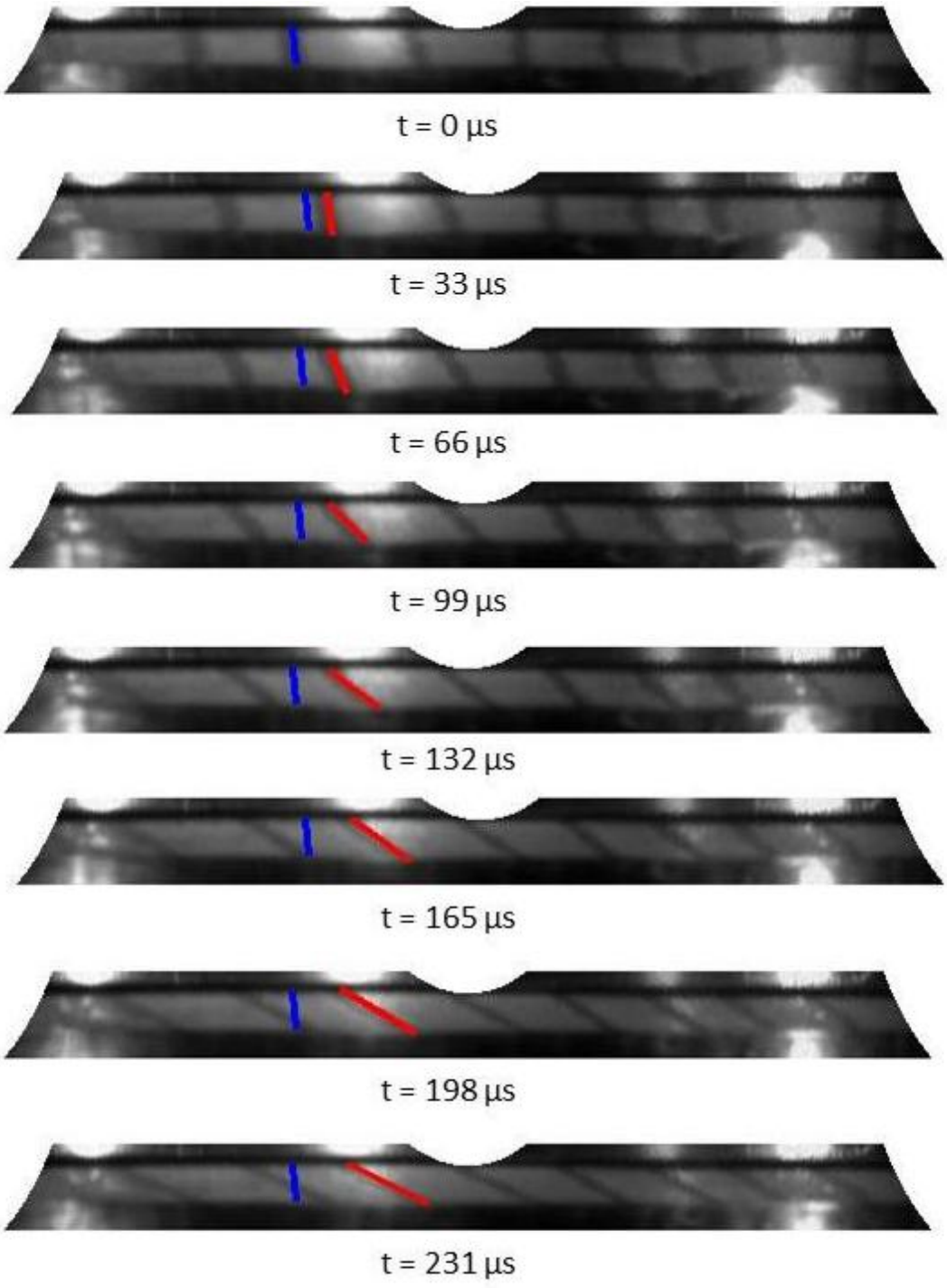

Figure 4.15: 1100-O Aluminum Unwrapped Images

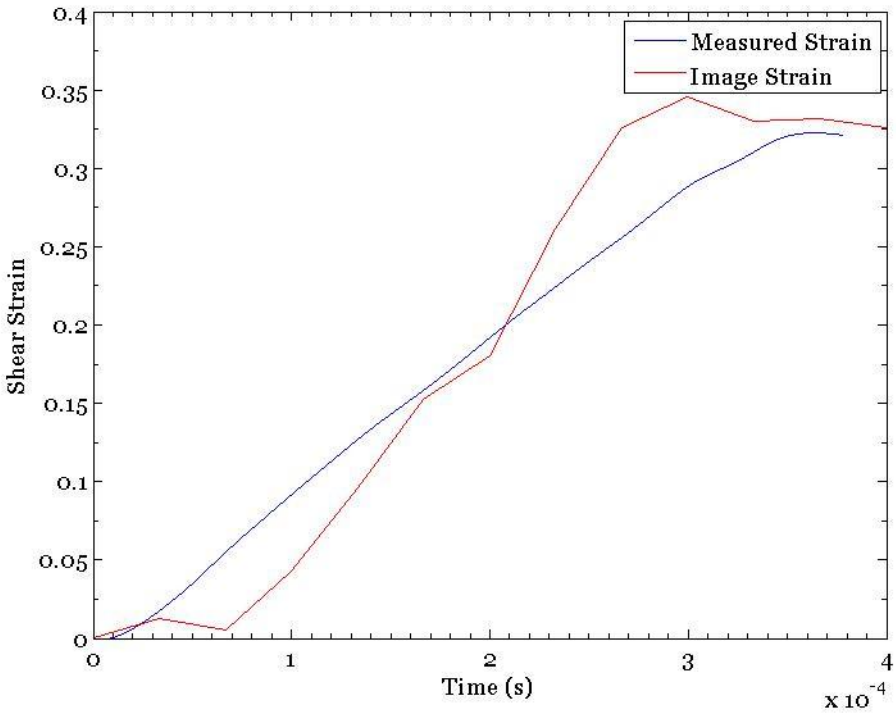

Figure 4.16: 1100-O Aluminum Strain Measurement Comparison

Chapter 5: Conclusions and Recommendations

The objective of this study was to construct a torsional Kolsky bar and optical measurement system to investigate the behavior of 6061-O and 1100-O aluminum under high strain rate shear loading. A summary of the operation of the torsional Kolsky bar presented in Chapter 2 led to the design and construction of the bar described in Chapter 3. This was followed by the design and fabrication of the aluminum specimens. A total of twelve experiments were conducted on 6061-O and 1100-O aluminum specimens of varying outer diameter, wall thickness, and gage length. The experimental data were analyzed to produce the results presented in Chapter 4. This section provides a summary of the conclusions of this study as well as some recommendations for future study.

The results for the 6061-O aluminum specimens agreed with known values, demonstrating the successful operation of the constructed torsional Kolsky bar. Applying the conical mirror and high speed camera to visualize the surface shear strains of specimens tested by the torsional Kolsky bar produced easily attainable qualitative results. However, converting the visualized angles to the specimen shear strains depends on a geometric conversion factor that is sensitive to the dimensions of the specimen as well as the relative position between the specimen and conical mirror.

The results for the 1100-O aluminum specimens conformed to the expected strain rate dependence but diverged from the shear stress – shear strain behavior observed by Gilat (1988). Possible explanations for this discrepancy include that the 1100-O aluminum was obtained ‘as-is’ from a supplier and its heat treatment was not confirmed in-house. The resulting stress-strain behavior may be due to the specimens being made from an 1100 aluminum alloy with an unknown heat treatment. In addition, when

machining the 1100 aluminum it was difficult to create smooth surfaces as the material was soft and would peel rather than cut cleanly. The resulting specimens may have introduced errors in the measurement due to their non-uniformity. The addition of real time viewing through the high speed camera allowed the propagation of the wave through the specimen to be seen. The ultimate goal of this capability is to observe the formation of shear bands when the specimen is subjected to sufficiently large strains, which did not occur during the course of this study.

Recommendations for further study include modifying the torsional Kolsky bar to store larger torques to generate greater strains in specimens. To accomplish this, the clamping mechanism could be adapted to clamp onto flat sections cut into the loading bar. This would reduce dependence on the friction between the clamp and the bar, eliminating unwanted slipping. To increase the duration of the pulse, the input and output bars would need to be made longer to accommodate a longer loading bar section. Increasing the outer diameter of the input and output bars would permit the use of shorter specimens with larger diameters. When used in conjunction with the conical mirror, images with greater clarity would be produced.

Appendix A: Torsional Kolsky Bar Component Schematics

The following figures show the specifications used in the design and manufacture of the torsional Kolsky bar used in these experiments.

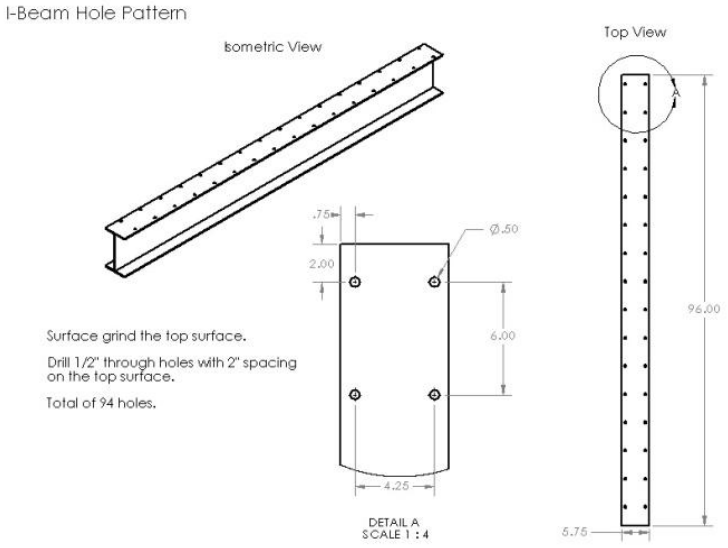

Figure A.1: I-Beam Support Schematic

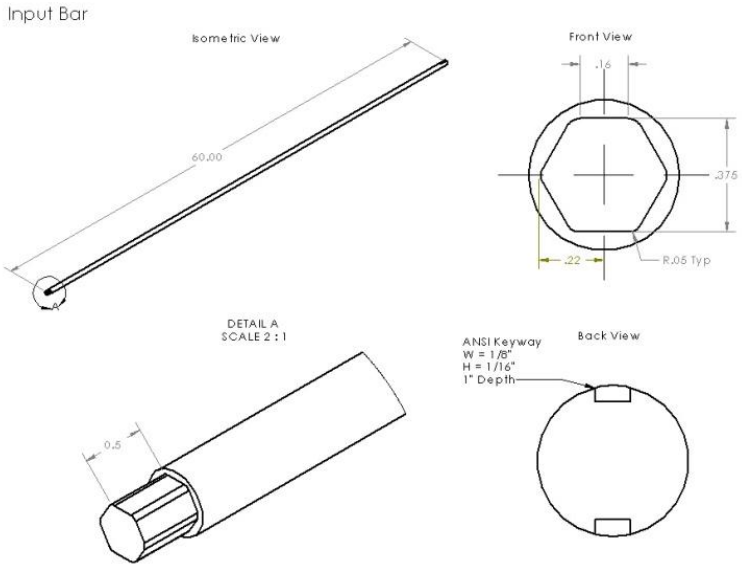

Figure A.2: Input Bar Schematic

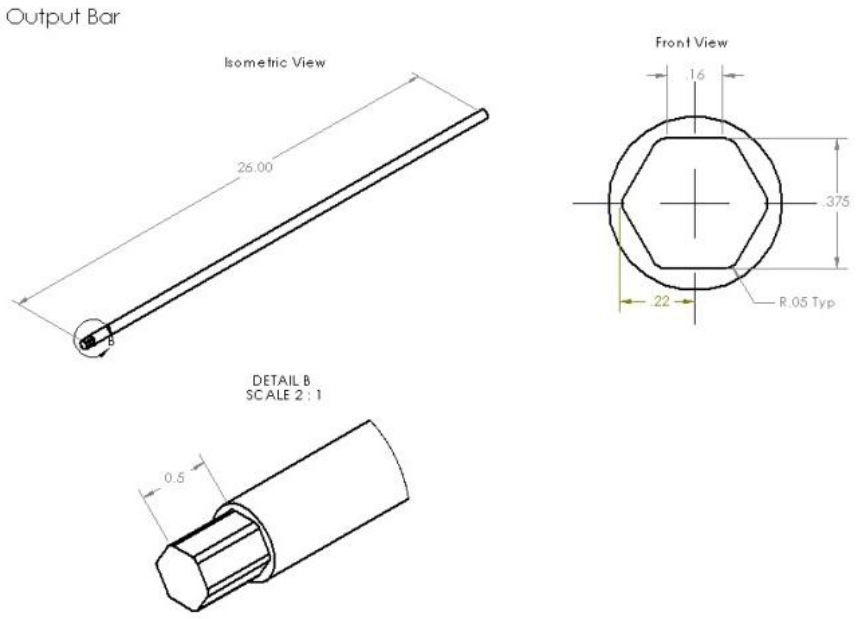

Figure A.3: Output Bar Schematic

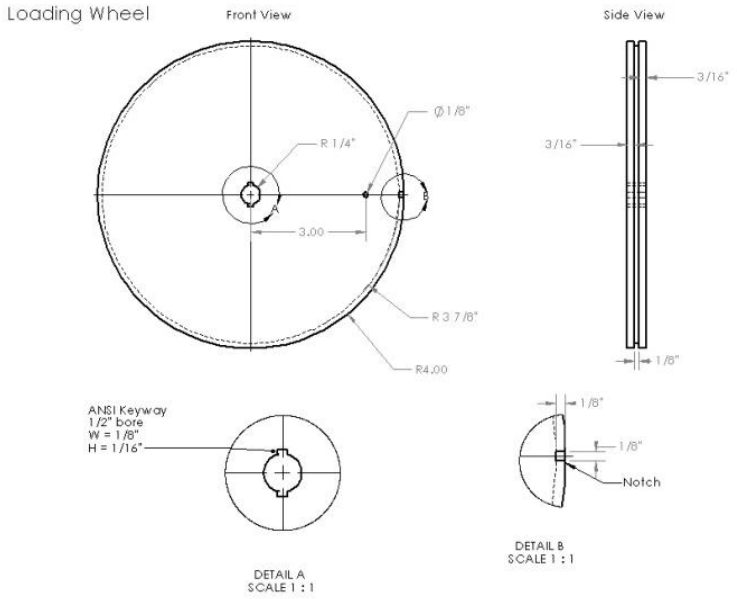

Figure A.4: Loading Wheel Schematic

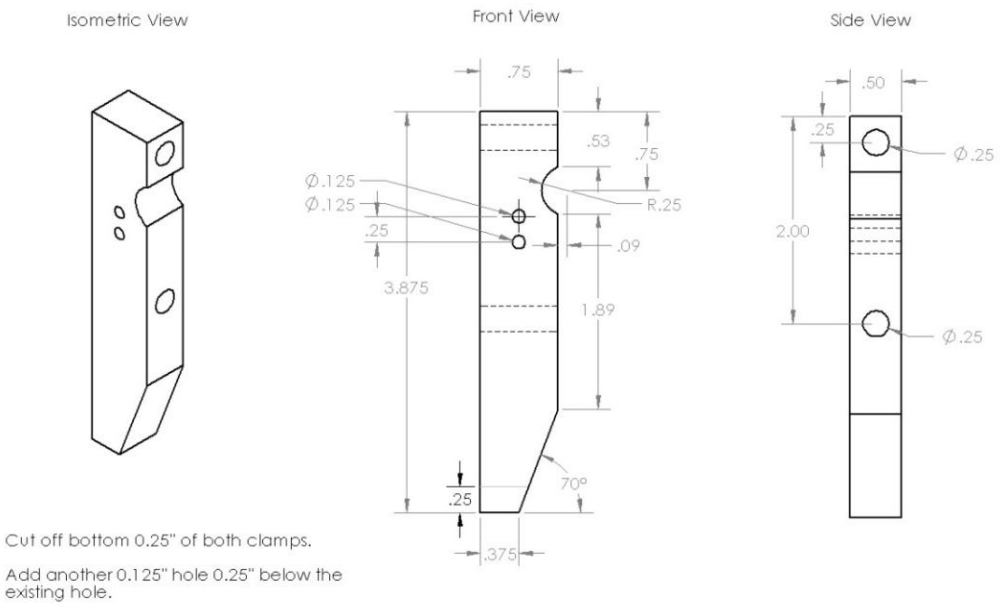

Figure A.5: Clamp Arm Schematic

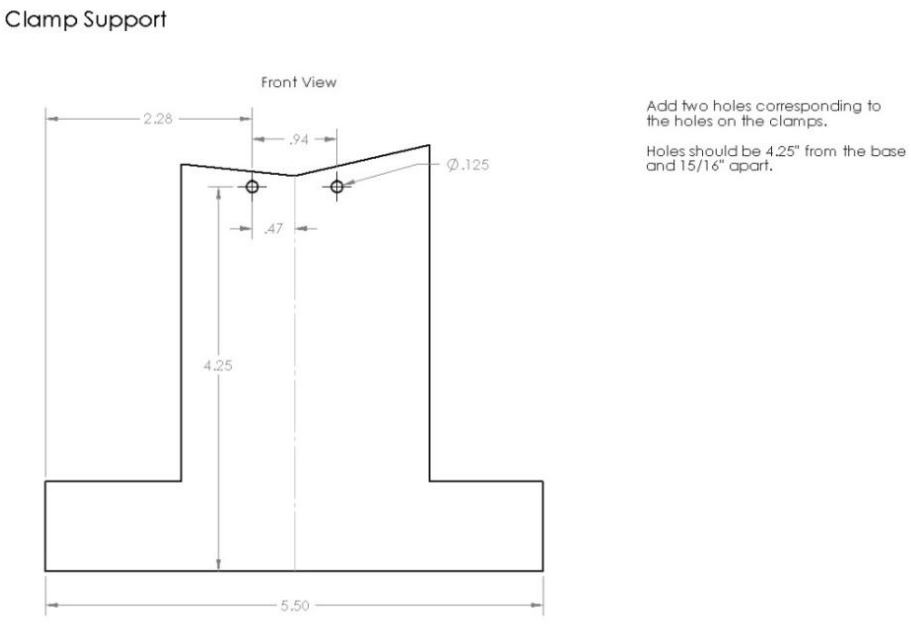

Figure A.6: Clamp Support Schematic

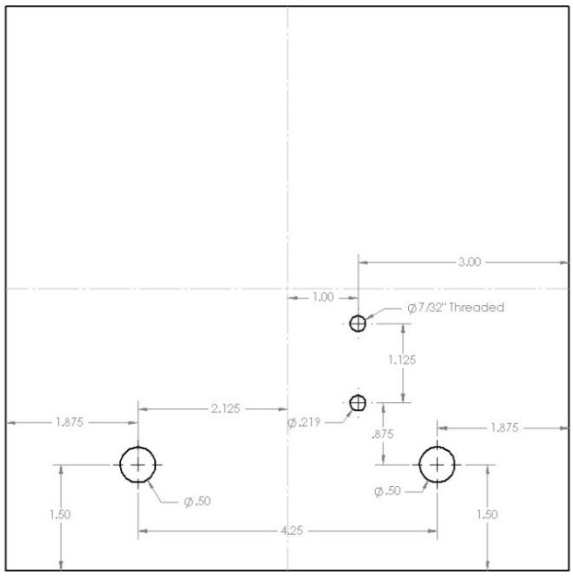

Figure A.7: Clamp Base Support Schematic

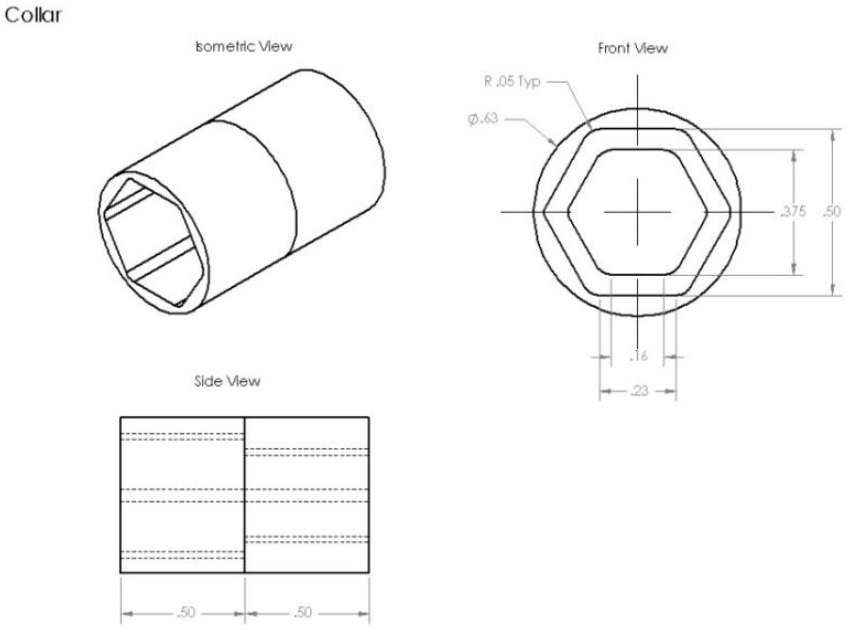

Figure A.8: Collar Schematic

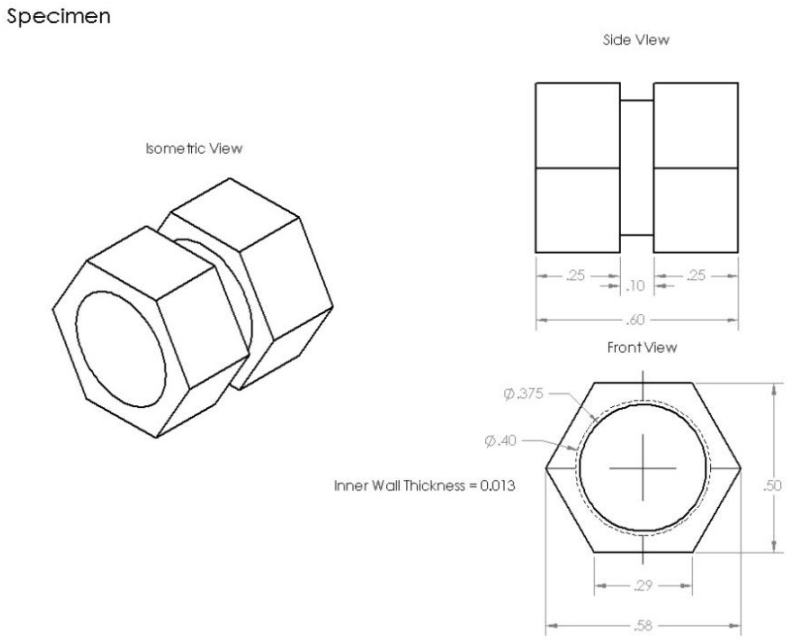

Figure A.9: Specimen Schematic

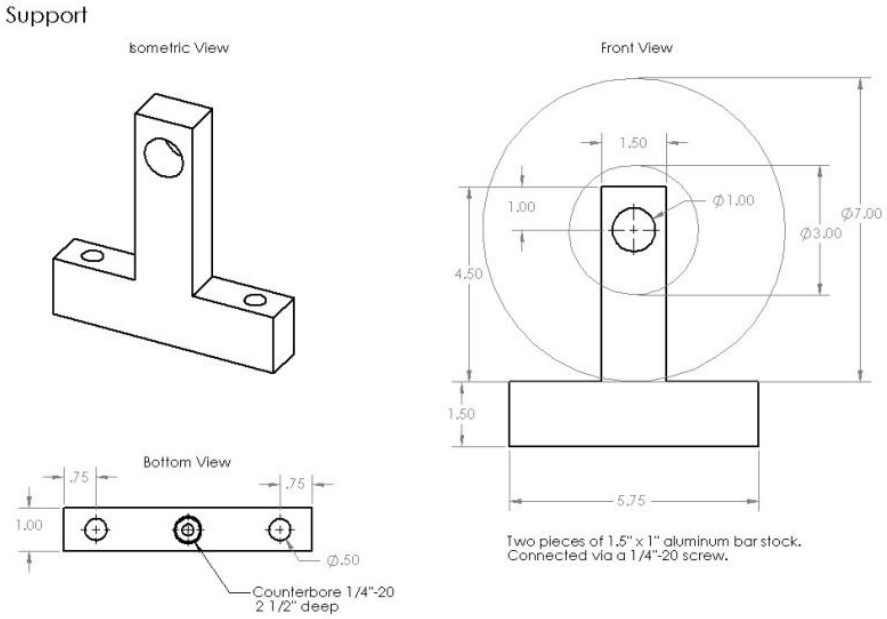

Figure A.10: Bar Support Schematic

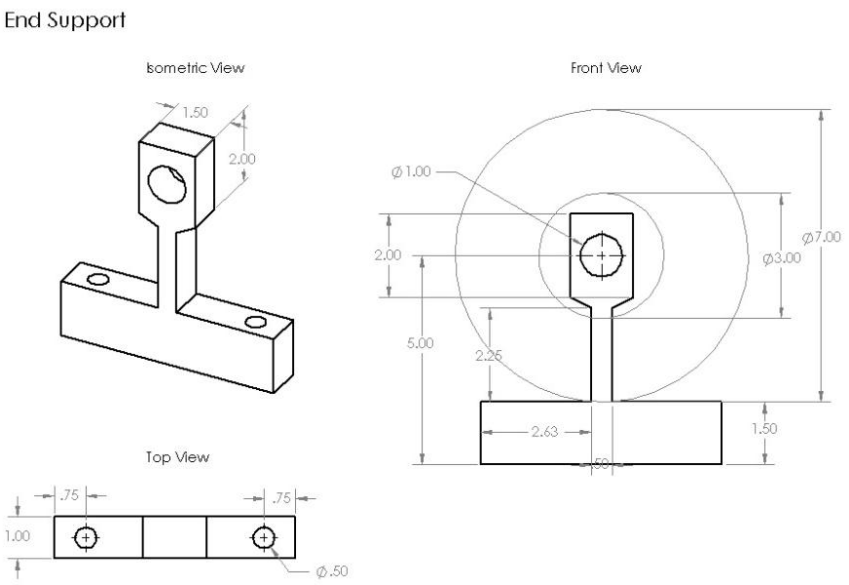

Figure A.11: Bar End Support Schematic

Appendix B: MATLAB Scripts

This section contains the MATLAB scripts written to compute the design parameters and process the collected results.

Code B.1: ImpedanceCalc

The following function was written in MATLAB in order to compute the transmitted torque required, transmission coefficient, and stored torque required for a specimen and input bar of arbitrary material composition and dimensions.

```
% Impedance Matching Calculation
% M1 = Bar Material
% M2 = Specimen Material
% 1 = Aluminum, 2 = Polycarbonate, 3 = Steel
% Db = Bar Diameter (inches)
% Dis = Specimen Inner Diameter (inches)

function ImpedanceCalc(M1,M2,Dob,Dis)

% Material Selection
mat = [M1 M2];    % [bar specimen]
for i = 1:length(mat)
    if mat(i) == 1  % Aluminum 6061-T6
        p(i) = 2.7e3;
        E(i) = 70e9;
        G(i) = 26e9;
        v(i) = 0.35;
        c(i) = sqrt(G(i)/p(i));
        tauy(i) = 207e6;
        mname(i) = cellstr('Aluminum');
    elseif mat(i) == 2    % Polycarbonate
        p(i) = 1.2e3;
        E(i) = 2.4e9;
        G(i) = 0.85e9;
        v(i) = 0.37;
        c(i) = sqrt(G(i)/p(i));
        tauy(i) = 36e6;
        mname(i) = cellstr('Poly');
    elseif mat(i) == 3    % Steel
        p(i) = 7.85e3;
        E(i) = 150e9;
        G(i) = 80e9;
        c(i) = sqrt(G(i)/p(i));
        tauy(i) = 462e6;
        mname(i) = cellstr('Steel');
    elseif mat(i) == 4  % Aluminum 1100-O
        p(i) = 2.7e3;
        E(i) = 68.9e9;
```

```
        G(i) = 26e9;
        v(i) = 0.33;
        c(i) = sqrt(G(i)/p(i));
        tauy(i) = 62.1e6;
        mname(i) = cellstr('Aluminum');
    end
end

Do(1) = Dob*.0254;
Di(1) = 0;
Di(2) = Dis*.0254;

taus = 100e6;    % Desired shear stress in specimen (MPa)

% Vary the outer diameter of the specimen
for i = 1:75
    Do(2) = Di(2)+0.0001*i;    % Outer Diameter 2 (m)
    Dos(i) = Do(2);
    t(i) = 0.5*(Do(2)-Di(2));
    r = 0.25*(Do(2)+Di(2));
    for k = 1:2
        Ip(k) = pi/32*(Do(k)^4-Di(k)^4);
        Z(k) = p(k)*c(k)*Ip(k);
    end



    Tt(i) = (2*taus*Ip(2))/Do(2); % Transmitted torque required (N*m)
    Zt(i) = (2*Z(2))/(Z(1)+Z(2));     % Transmission Coefficient
    Ti = 1/Zt(i)*Tt(i)/2;     % Incident torque required (N*m)
    Ty(i) = 2*tauy(1)*Ip(1)/Do(1);   % Yield torque of the bar (N*m)
    gamy(i) = tauy(1)/G(1)*1000;
    Tbar(i) = 2*Ti;    % Torque stored in bar (N*m)
    taub(i) = Tbar(i)*Do(1)/(2*Ip(1));       % Shear stress in bar (Pa)
    tauys(i) = tauy(2);

    gamb(i) = taub(i)/G(1)*1000; % milli Strain
end
```

Code B.2: KolskyDriver

The following code was written in MATLAB in order to calculate the shear stress and shear strain in the specimen from the provided data recorded by the strain gages during the experiment.

```
% Select the correct test to obtain specimen dimensions
date1 = 4;
date2 = 25;
test = 2;

data = csvread('TestData.csv',1,0);
daterange = find(data(:,2)==date2);
testrow = find(data([daterange],3)==test);

% Initialize the dimensions of the specimen
Do = data(daterange(testrow),5)*.0254;
Di = data(daterange(testrow),4)*.0254;
Ls = data(daterange(testrow),6)*.0254;

testname = [num2str(date1) num2str(date2) num2str(test) '.CSV'];
data = csvread(testname,15,0);      % Read the waveform data
time = data(7000:35000,1);          % Time data
ch1 = data(7000:35000,2)/1000*2;    % Stored torque value
ch2 = data(7000:35000,3)/1000*2;    % Incident and reflected wave data
ch3 = data(7000:35000,4)/(-1000)/2*2;    % Transmitted wave data

samplestep = time(2)-time(1);    % Time between samples in seconds

G = 26e9;        % Kolsky Bar Shear Modulus (Pa)
density = 2.7e3;     % Density of the aluminum bar (kg/m^3)
c = sqrt(G/density);     % Shear wave speed of the bar (m/s)
Ds = (Do+Di)/2;     % Average diameter of the specimen (m)

D = 0.5*.0254;       % Diameter of the bar (m)
ts = (Do-Di)/2;    % Thickness of the specimen (m)

lcg1 = 21*.0254;     % Distance between clamp and gage 1 (incident)
lpulse = 2*14.5*.0254;


% Determine the start time of the stress wave for each gage
a = find(ch1<0.87*ch1(1),1,'first'); % Start of release in ch1
```

```
starttime = time(a) - (10.5*0.0254)/c;
b = find(ch2<-2.4e-4,1,'first')+0; % Start of incident pulse in ch2
g2itimea = time(b);
g2itimec = lcg1/c+starttime;
g2rtimec = (lcg1+2*24.5*0.0254)/c+starttime;
pulselength = floor(1.6*lpulse/c/samplestep);
d = b+pulselength; % End of incident pulse in ch2
e = find(ch3<-1e-4,1,'first'); % Start of transmitted pulse in ch3
f = e+pulselength; % End of transmitted pulse in ch3
g = find(time>0.82*g2rtimec,1,'first');% Start of reflected pulse in
ch2
h = g+pulselength; % End of reflected pulse in ch2
if h > length(ch2)
    h = 0.96*length(ch2);
    g = h-pulselength;
end

gammai = ch2(b:d);     % Incident shear strain
gammar = ch2(g:h);     % Reflected shear strain
gammat = ch3(e:f);     % Transmitted shear strain
timer = time(g:h);     % Time of reflected wave
timet = time(e:f);
gammarmax = max(gammar(1500:length(gammar)));

gammasr = 2*c*Do*gammar/(Ls*D); % Specimen shear strain rate

shears = -G*D^3*gammat*Do/(Do^4-Di^4); % Specimen shear stress
gammas = zeros(length(timer),1);     % Specimen shear strain

ShearActual = max(shears)

% Integrate the strain rate to obtain specimen shear strain
for i = 2:length(timer)
    gammas(i) = trapz(timer(1:i),gammasr(1:i));
end

% Convert to true stress and strain
nomstrain = gammas/sqrt(3);
truestrain = log(1+nomstrain);
nomstress = shears*sqrt(3);
truestress = nomstress.*(1+nomstrain);

% Ramberg-Osgood Fit
beta = 14165;
n = 0.22;
yieldstress = 25e6;
plasticstrain = linspace(0,0.18,100);
truefitstress = yieldstress*(1+beta.*plasticstrain).^n;
```

Code B.3: UnwrapMappingScript

The following code was written in MATLAB to convert the images of the conical mirror recorded by the Photron images into a mapping of the specimen surface in rectangular coordinates.

```
%[serial, qc, pc, Dt, Dm, hm]=textread('imageinfo.txt','%s %f %f %f %d
%d','headerlines',1);
Where: serial refers to the image name,  qc and pc are the center of
the tube pixel location, dt is the outer diameter of the tube, dm is
the mean diameter of the image of the tube in the mirror, hm is the
"height" of the image in the mirror
testname = '4_10_3';
totname = [testname '_Images/'];

% Select the desired range of images to read
for k = 0:0
    for i = 0:9
        for j = 0:9
            if i == 0 && j == 0 && k == 0
            else
                serial(count,:) = [num2str(k) num2str(i) num2str(j)];
                count = count + 1;
            end
        end
    end
end

amp_width = 1.188; % factor used to correct distortion due to camera
lens

angle = 40*pi()/180; % should be 40*pi()/180, see schematic for
clarification

% Create a video of the images
% Prepare the new file
vidObj = VideoWriter([totname testname '_map1.avi']);
vidObj.FrameRate = 5;
open(vidObj);


nframe = size(serial,1);
for i=1:nframe
    fid= char(strcat(serial(i,:), '.bmp'));
```

```
    frame = imread([totname fid], 'bmp');

    h = hm;
    q0 = qc;
    p0 = pc;

    rt = Dt/2;
    rm = Dm/2;
    r1 = rm - h/2;
    r2 = rm + h/2;

    w = round(h/cos(angle)*amp_width);
    u = round(2*pi()*rt);

    map=255*ones(w+1,u+1);

    for m = 1:w+1
        for n = 1:u+1
            theta = (n-1)*2*pi()/u-pi/3;
            r = r1 + h*(w-(m-1))/w;
            p = p0 - r*sin(theta);
            q = q0 - r*cos(theta);
            if p>=1 && q>=1 && p<240 && q<320
                p1 = floor(p);
                p2 = ceil(p);
                q1 = floor(q);
                q2 = ceil(q);
                xi = -1 + 2*(p-p1);
                eta = -1 + 2*(q-q1);
                N1 = (1-xi)*(1-eta)/4;
                N2 = (1+xi)*(1-eta)/4;
                N3 = (1+xi)*(1+eta)/4;
                N4 = (1-xi)*(1+eta)/4;
                map(m,n) =
N1*frame(p1,q1)+N2*frame(p2,q1)+N3*frame(p2,q2)+N4*frame(p1,q2);
            else
                map(m,n) = 255;
           end
        end
    end
    fod = char(strcat(serial(i,:), '-map.tif'));
    total = [totname 'processed/' fod];
    imwrite(uint8(map), total, 'tif');
    image = imread(total, 'tif');
    writeVideo(vidObj,image);
end

close(vidObj);
```

Code B.4: AngleMeasurement

The following code was written in MATLAB in order to measure the change in angle between the processed images. This angle measurement was then converted into shear strain through the use of a geometric scaling parameter.

```
% Select the images from the correct test
month = 4;
date = 10;
testnum = 3;

testname = [num2str(month) '_' num2str(date) '_' num2str(testnum)];
totname = [testname '_Images/'];

data = csvread('TestData.csv',1,0);
daterange = find(data(:,2)==date);
testrow = find(data([daterange],3)==testnum);
r = data(testrow,5)/2*.0254;
L = data(testrow,6)*.0254;

count = 1;
for k = 0:0
    for i = 0:1
        for j = 0:9
            if i == 0 && j == 0 && k == 0

            elseif i == 0 && j >= 3
                serial(count,:) = [num2str(k) num2str(i) num2str(j)];
                count = count + 1;
            elseif i == 1 && j <= 5
                serial(count,:) = [num2str(k) num2str(i) num2str(j)];
                count = count + 1;
            end
        end
    end
end


nframe = size(serial,1);

% Angle Measurement Script
for i=1:nframe
    name = figure(i);
    fid= char(strcat(serial(i,:), '-map.tif'));
```

```
    frame = imread([totname 'processed/' fid], 'tif');
    imshow(frame)

    hold on
    [x y] = ginput(2);
    plot(x,y,'r','Linewidth',3)
    if i == 1
        x0n = x(1);
        x1n = x(2);
        y0n = y(1);
        y1n = y(2);
    end
    x = x*2*r*pi/12;    % Width scaling
    y = y*L;            % Length scaling
    time(i) = (i-1)*33.3e-6;
    if i == 1
        x0 = x(1);
        x1 = x(2);
        y0 = y(1);
        y1 = y(2);
        magn1 = sqrt((x1 - x0)^2+(y1 - y0)^2);
        strain(1) = 0;

    else
        magn2 = sqrt((x(2) - x(1))^2+(y(2) - y(1))^2);
        dotp = (x1-x0)*(x(2)-x(1))+(y1-y0)*(y(2)-y(1));
        angle(i) = acos(dotp/(magn1*magn2));
        strain(i) = angle(i);
    end
    plot([x0n x1n], [y0n y1n],'b', 'Linewidth',3)

end

figure
plot(time(1:nframe),strain(1:nframe))
xlabel('Time (microseconds)')
ylabel('Shear Strain)
```

References

Culver, R. S., Torsional Impact Apparatus, *Experimental Mechanics*, Vol. 12, 1972, 398-405

Duffy J., Campbell J. D., Hawley R. H., On the Use of a Torsional Split Hopkinson Bar to Study Rate Effects in 1100-O Aluminum, *Journal of Applied Mechanics*, 1971, 83-91

Duffy J., Marchand A., An Experimental Study of the Formation Process of Adiabatic Shear Bands in a Structural Steel, *Journal Mechanical Physics Solids* Vol. 36, No. 3, 1988, 251-283

Gilat A., Torsional Kolsky Bar Testing, *Mechanical Testing and Evaluation,* Vol 8, *ASM Handbook*, ASM International, 2000, 505-515

Gilat A., Pao Y. H., High-Rate Decremental-Strain-Rate Test, *Experimental Mechanics,* September 1988, 322-325

Gilat A., Cheng C. -S., Torsional Split Hopkinson Bar Tests at Strain Rates above 10^4 s^{-1}, *Experimental Mechanics*, Vol. 40, No. 1, 2000, 54-59

Graff K. F., Wave Motion in Elastic Solids, *Courier Dover Publications*, 1975

Lindholm U. S., Nagy A., Johnson G. R., Hoegeldt J. M., Large Strain, High Strain Rate Testing of Copper, *Transactions of the ASME* 1980, Vol. 102, 376-381

Zhang H., Ravi-Chandar K., On the dynamics of localization and fragmentation-IV. Expansion of Al 6061-O tubes, *International Journal of Fracture*, Vol. 163, 2010, 41-65

Vita

Stephen Vargo Williams was born on June 2nd 1989. He graduated from Carroll Senior High School in 2007. He received a Bachelor of Science in Mechanical Engineering from Rice University in May 2011. He attended The University of Texas at Austin beginning in August 2011 pursuing a Master of Science degree in Aerospace Engineering.

Permanent email address: stephen.v.williams@utexas.edu

This thesis was typed by the author.